MEDICAL PHYSICS PUBLISHING

Here is a sample chapter from this book.

Chapter 31
Post Implant Evaluation

William S. Bice, Jr., Ph.D.
University of Texas Health Science Center at San Antonio
International Medical Physics Services
San Antonio, Texas

Introduction

Only the most irresponsible implant team would enter an operating room without a plan. This plan could be a formal one, calculated, printed, and approved by the physician, or could be as informal as an envisioned ideal procedure, based on the anatomy of the patient and the practiced skill of the brachytherapist. But, no matter how skilled the physician, how practiced the team, how ideal the patient, the implant never, ever matches the plan. Properly performed afterloading techniques, e.g., high dose-rate (HDR) procedures, are less affected by this discrepancy than implants performed entirely during the operative procedure, e.g., permanent prostate brachytherapy. In the case of seed implants this has been the impetus for in-OR (in-operating room) treatment planning and in-OR dosimetry. Post-operative evaluation of the implant can then be defined as narrowly as that performed after the entire procedure or as broadly as any analysis performed after placement of the delivery apparatus, for example, afterloading catheters or gynecological applicators.

In this chapter the analysis is restricted to the more narrow definition: post-implant evaluation is analysis performed after the implant has been completed and the radiation dose delivered (or seeds have been implanted). Dosimetry and design performed after the applicators are in place is considered part of the implant procedure, and has been described in other chapters of the monograph.

So if we restrict post-implant evaluation to the analysis performed after the procedure is finished, why do it? The radiation dose cannot be taken back; looking afterward only invites trouble! There are two compelling reasons for conducting post-implant evaluation. Clearly, the quality of the implant needs to be evaluated to determine if there is any need for additional treatment or if unwanted complications might result. Just as importantly however, the implant should be evaluated in terms of the quality of the procedure itself: a measure of the performance of the implant team. This is more than an evaluation of the skill of the physician. Post-implant evaluation should include the adequacy of the implant design, skill of the operating room staff, and appropriateness of the equipment used in the procedure. Nothing contributes to making the next implant better like reviewing the last twenty.

Most post-implant evaluation is performed to assess permanent prostate brachytherapy (PPB) procedures. This will, of necessity then, be the slant of this chapter. It does not mean that the same methods cannot be used to evaluate other types of implants. What procedure would not be improved by a detailed review of dose delivered, the patient outcome, and the techniques employed? But it is in PPB that the need for formal post-implant planning and procedural evaluation first became apparent. The gains were immediate and dramatic. A series of brachytherapy “tools” were developed to aid in, or due to, post-implant analysis for PPB. Ultrasound and computed tomography (CT)-based three-dimensional (3-D) imaging, automated source identification and localization, refinement and development of implant quantifiers, electronic transfer formats, and standards for brachytherapy all came about because of the success and popularity of PPB. The street is traveled in two directions: no treatment modality has seen such rapid, widespread improvement due to the development of quality evaluation tools. PPB and post-implant evaluation were made for each other; each getting better, feeding off the successes of the other.

Background

Films for Record

Fifteen years ago meaningful post-implant dosimetry did not exist. The best that most clinical physicists could offer was something called “films for record”. This usually consisted of a single radiograph, or at best a pair of radiographs, taken on a simulator, which showed little more than source locations and bony anatomy. These we dutifully filed in the patient’s film jacket along with the physician’s note, confident that we had, indeed, performed the implant. How depressingly inadequate!

Paired Film Localization

Of course, one could perform source localization from a pair of films or, even better, a triplet. Most treatment-planning systems, even those primarily dedicated to external-beam planning (this was all of them during this time) had the capacity to localize points and sources from a paired film set. This was primarily to satisfy the demand for gynecological brachytherapy planning; five or six large sources in a more or less fixed geometry with a relatively fixed set of four or five calculation points. Using this system to identify and localize a prostate implant with 100 seeds was euphemistically described as burdensome. Nevertheless, it was possible, and one could generate isodose planes, or even clouds, to depict the distribution of radiation dose.

Without anatomical reference, of course, the information from paired-film dosimetry is really of little more use than from films for record. More information to file in the patient's record, this time convincing ourselves that, not only did we perform the implant, but there was also radiation involved.

This is not to say that source localization from paired films is useless. Paired film localization is still in use today and, rightfully, a topic in this book. But the best use of this technique has become in conjunction with another imaging modality, usually tomographic—one that depicts soft tissues. Fusing the source information from the paired radiographs with the soft-tissue imaging modality marries the dose and structures, essential for determining the quality of the implant.

Meaningful Post-Planning

Post-planning then is a function of the imaging modality and the treatment-planning system. Post-implant evaluation performed without meaningful post-planning is an empty process, drawing conclusions with no data. Characteristics of meaningful post-planning include:

1. the use of tomographic imaging modalities with automated source localization capabilities;
2. performance of 3-D calculation, analysis and, preferably, display;
3. calculation and analysis based upon localized structures—targets and critical structures;
4. a calculation grid size that is appropriately small enough to distinguish dosimetric changes over either small volumes of interest or in areas of rapidly changing dose;
5. structure-based dose-volume or dose-surface analysis with sufficient sampling of dose within the structure to meet statistical requirements; and
6. implant quantifier determination.

Imaging

Plane Radiography

Fluoroscopy and radiography have been used in the post-implant setting. The lack of anatomical information is clearly a significant drawback. As described above paired films or, alternatively, multiple-projection fluoroscopy can be used to determine source locations (Tubic et al., 2001; Tutar et al., 2003; Narayanan et al., 2004; Su et al., 2004). A plane radiograph can always be taken to verify the number of sources in an implant. This is especially important for prostate brachytherapy, where the sources may migrate within, sometimes eliminated from, the patient (Merrick et al. 2000a). Visibility of the sources depends on the source configuration and the marker type. Plane films may be used in conjunction with modalities where sources appear on multiple images and the source count may be required to reliably

reduce the available source positions to true source locations. Seed sorting will be discussed later in this chapter.

Computed Tomography (CT)

The first published use of CT for post-implant dosimetry was in the early 1990s at Memorial Sloan-Kettering Cancer Center (Roy et al., 1993b). Structures and sources were localized on the axial image sets and this information fed into the in-house planning system. This was the first display of organ and dose location together for post implant dosimetry. It soon became apparent that the concept of designing implants based upon matched peripheral dose (MPD), where choosing a reference dose volume to match the volume of the gland, was inadequate. Post-implant evaluation quickly achieved its intended purpose: provide enough feedback to the implant team to allow them to change the design and delivery system to perform better implants.

By far, the majority of the post-implant imaging performed today is CT based. CT units are ubiquitous in radiotherapy, the expense is relatively low, and the source locations are easily visualized. Almost the entire experience in the medical community with evaluating the quality of post-implant dosimetry is based upon CT. The lack of ability to visualize the glandular borders clearly, particularly in the edematous post-implant patient, is disconcerting. Large uncertainties exist in the results because of the uncertainties in glandular borders. The variance of the post-implant dosimetry due to the inability to clearly delineate the prostate gland appears to be related to implant quality; better implants have less dependence on visualization of the gland (Bice et al., 1998; Merrick et al., 1999b; Lee et al., 2002; Crook et al., 2002; Lindsay, Van Dyk, and Battista 2003; Han et al., 2003b).

The imaging sequence used to generate the tomographic CT-image set varies widely among practitioners. Scan parameters are usually chosen based upon the ability to best determine source locations. This means a reduced field of view, usually about 15 cm, just large enough to encompass the meaningful dose regions and the critical structures. Slice spacing varies from 1 mm to 5 mm; slice width also varies from that which provides abutting slices to something smaller (1-mm slices at 5-mm spacing, for example). When detecting 4.5-mm sources with "random" orientations, 5-mm spacing between slices is almost certainly under sampling, resulting in unwanted uncertainties with regard to localization and subsequent dosimetry. The reasons for such large spacing, elimination of the source location redundancy problem (seed sorting), and general time savings with regard to contouring and location of the sources on each slice, have been adequately addressed with modern planning systems (Brinkman and Kline 1998; Bice et al., 1999; Li et al., 2001; Liu et al., 2003; Davis et al., 2004; Lam et al., 2004; Holupka et al., 2004). Automated detection and seed sorting, combined with the ability to interpolate contoured structures obviates the need for the introduction of such uncertainties. Although no rigorous study pertaining to the choice of CT imaging sequence has been published, source location uncertainties can dramatically affect the dosimetric analysis and possibly the biological outcome (Lindsay, Van Dyk, and Battista 2003). Slice spacing greater than 3 mm is not recommended (Nag et al., 2000).

The effect on source location of acquiring the CT image set with helical scans as opposed to axial scans is similarly unstudied but seems to make little difference clinically.

Magnetic Resonance Imaging (MRI)

CT provides excellent visualization of the sources, but very poor delineation of the soft tissue boundaries. Magnetic resonance imaging (MRI), with excellent soft tissue contrast, has also been used for post-implant imaging (Moerland et al., 1997; Dubois 1999; Dubois et al., 1998). The ability to visualize glandular borders, particularly at the base and apex of the gland, is of significant advantage. A pelvic coil is much preferred to an endorectal coil, as the latter tends to cause great discomfort in the post-operative patient.

For MRI, several authors have published viable imaging sequences (Dubois 1999; Amdur et al., 1999; Kooy et al., 2000; McLaughlin et al., 2002; Polo et al., 2004). A reduced field of view, similar to CT, is always used. Scans may be acquired with sequences that provide T1- or T2-weighted images. Care must be taken to ensure image distortion in MR data acquisition is kept to a minimum. A comprehensive quality assurance (QA) program is a must.

Dosimetry based upon MRI alone, however is probably inadequate due to the inability to distinguish source locations—which do not image—from other objects which show up as holes: blood vessels, calcifications, spacers. Source localization methods based on MRI alone tend to reduce the distance between implanted sources, drawing the isodose volumes in toward the center of the implant (Dubois et al., 1997; Prete et al., 1998). Dubois and Davis have done some work with regard to developing an MR-visible source by doping the source with paramagnetic elements (Dubois 1999, Davis et al., 2004).

Other Imaging Modalities

Glandular borders are readily imaged with ultrasound. Tomographic image sets, collected in either axial or parasagittal directions, can be used to build up 3-D images. The use of a rectal ultrasound probe is uncomfortable, of course, and the use of ultrasound for post-implant imaging has been mostly limited to acquisition in the OR following the procedure while the patient is still anesthetized. The real issue with regard to using ultrasound for post-implant dosimetry is the inability to perceive source locations on the ultrasound image. One manufacturer sells an echogenic source, but reliable post-implant dosimetry from an ultrasound image set using this source is not currently viable (Han et al., 2003a). Transurethral ultrasound has shown promise for delineation of the prostatic borders and seed localization but is currently limited to phantom studies (Holmes, Davis, and Robb 2001).

There has been some preliminary work done with positron emission tomography (PET) imaging of the sources (Sajo 2003). Although PET images metabolic activity, it has not been shown to be useful in prostate cancer. Single photon emission computed tomography (SPECT) using ^{111}In has had some success in imaging the disease both locally and as a measure of nodal or metastatic involvement (Sodee et al., 1998; Texter and Neal 1998; Fang et al., 2000; Ellis et al., 2003; Ellis, Kim, and Foor 2004; DeWyngaert et al., 2004). Additionally, anatomic information is only marginally visible on PET or SPECT images; fusion with CT is regularly used to localize the metabolic information.

MR spectroscopy (MRS) offers both anatomic information and localization of the disease (Zaider et al., 2000; Mizowaki et al., 2002; Claus, Hricak, and Hattery 2004). Again though, accurately visualizing the sources is difficult—requiring fusion of the MR and MRS image sets to CT.

Image Fusion

Various image fusion methods have been used in post-implant imaging. The idea is to co-register the image data from a modality in which the sources are clearly visible, like CT or fluoroscopy, with another modality that images soft tissue well, such as MRI or ultrasound. The advantages are clear; the major drawbacks are cost and patient trauma.

Of the available modalities, CT-MR fusion has been most extensively studied for post-implant dosimetry. See figure 3. Co-registration of the image sets has been performed by eye (Amdur et al., 1999) or by other more quantifiable and reproducible methods, such as available source locations (Dubois, Bice, and Prestidge 2001) or mutual information (McLaughlin et al., 2002; Tsai et al., 2004). Combining pre-implant volume study images with post-implant CT images has been employed by the Seattle group to help delineate the gland on CT (Badiozamani et al., 1999; Smith et al., 2003), but there is some debate as to the utility of this type of image fusion as edema resulting from the operative procedure clearly changes the structure of the prostate. Use of the pre-implant volume study to draw the gland on a post-implant CT

clearly underestimates the size of the gland, but the quantitative affect on coverage quantifiers appears to be small. This is shown in Figure 1. Ultrasound-CT fusion has been used successfully for post-implant evaluation and to perform planning for subsequent salvage therapy (Narayana et al., 1997; Bice et al., 2000). Ultrasound has also been fused to fluoroscopic projection imagery for prostate brachytherapy (Gong et al., 2002).

The cost of and time associated with acquiring and fusing two different image sets currently prohibits the use of image fusion on a routine basis, although recent developments in CT-US fusion may change this thinking. Several programs have found the use of CT-MR fusion valuable, performed in a selected number of cases, as a learning tool. The brachytherapist may use the MR to determine what changes need to be made in his CT-image-based contouring techniques (McLaughlin et al., 2002).

Image Timing: Edema

Various investigators have described the edematous change in the prostate gland during the operative procedure and post-implant resolution of the edema. Consequently, timing of post-implant image acquisition affects dosimetry. Imaging performed immediately post implant, also known as "day-0 imaging," results in lower doses being depicted on the post-implant treatment plan than imaging performed at any time thereafter. The typical change is shown in Figure 2. Several authors have shown that the most representative time to image the patient is 2 to 3 weeks following the procedure. Nevertheless day-0 imaging is still performed at many institutions, the advantages being immediate feedback and convenience for the patient. At institutions where a catheter is placed during the imaging procedure in order to be able to better localize the urethra, day-0 imaging precludes an additional catheter placement. Whatever time is chosen to perform the imaging procedure, it should be consistent. Analyzing a series of implants where the post-implant imaging procedure was performed at different times adds an unnecessary level of complexity and uncertainty to the results (Prestidge et al., 1998; Merrick et al., 1998; Willins and Wallner 1998; Yue et al. 1999a,b,c; Butler et al., 2000b; Speight et al., 2000; Waterman and Dicker 1999, 2000; Dogan et al., 2002).

Source Localization

Automated localization of sources in the tomographic image set, particularly for permanent prostate brachytherapy, has become essential for post-implant analysis. Covered elsewhere in this book, the source detection routine is divided into two parts: detection of source images on each slice and, since the sources may appear on more than one slice, reduction of the source image locations from all of the slices into possible source positions. The second task, also known as "seed sorting," is by far the more onerous to perform by hand. Multiple authors have provided automated solutions to both the problem of source image detection and seed sorting. The advantages of automation are not just limited to time savings. Having a logical and reproducible method of interpreting the information from the image set is paramount (Brinkman and Kline 1998; Bice et al., 1999; Li et al., 2001; Liu et al., 2003; Davis et al., 2004; Lam et al., 2004; Holupka et al., 2004).

Calculations and Analysis

Calculation Formalism

In February 1995, the recommendations of the AAPM task group formed to address problems with interstitial dosimetry were published (Nath et al., 1995). Commonly known simply as TG43, these recommendations provided a straightforward formalism for performing interstitial source dosimetry calcu-

Figure 1. Change in coverage quantifiers with change in glandular borders.

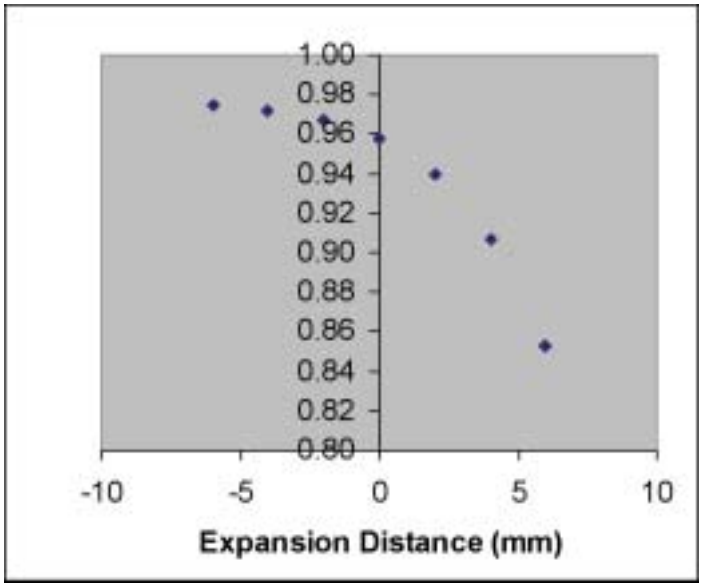

Figure 1.a. V_{100}.

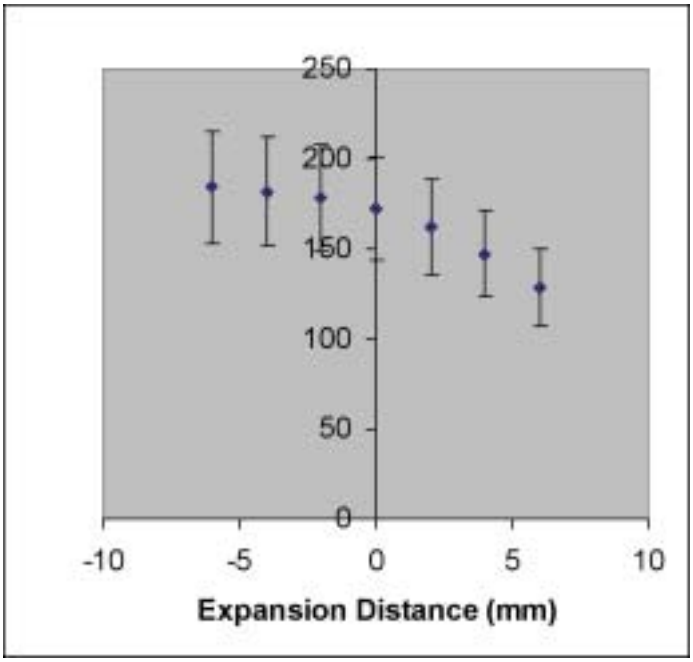

Figure 1.b. D_{90}.

Figure 1. The effect of misestimating gland size on post-implant imagery is shown in Figures 1a and 1b. In both figures the glandular borders for 50 implants were expanded and contracted by 2-mm increments, except in the posterior direction where the glandular border is most visible. In Figure 1a V_{100} is plotted, showing less change in V_{100} if the gland is drawn too small as compared to being drawn too large. A similar effect is shown on D_{90} in Figure 1b.

Figure 2. Change in volume and implant coverage due to edema.

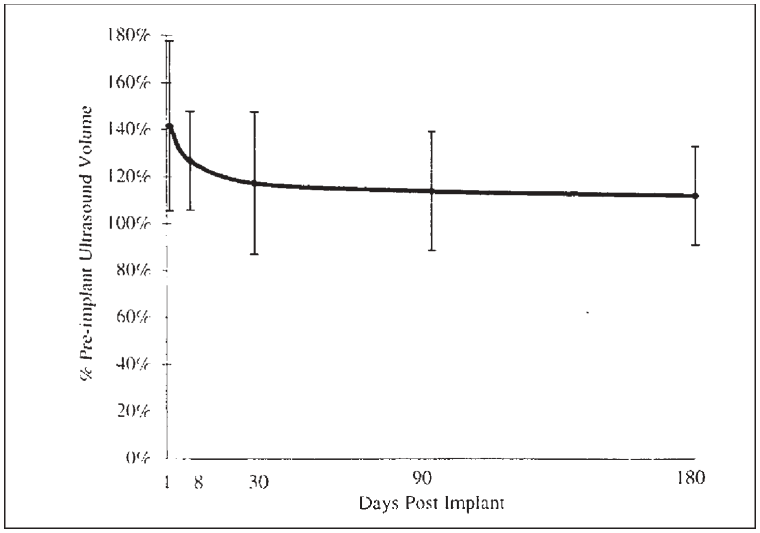

Figure 2.a. Change in volume with resolution of edema.

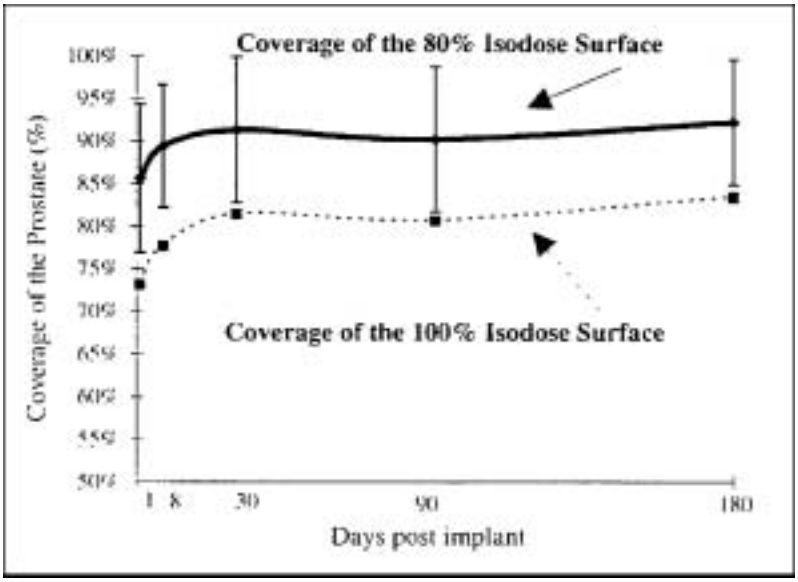

Figure 2.b. Change in coverage with resolution of edema.

This is data from 20 iodine monotherapy patients. The volume of the gland is reduced as the edema from the implant procedure resolves. The coverage of the gland correspondingly improves. Integrating the dose over the life of the implant indicates that the most representative time to image the gland is about day 25. Also note that these implants were performed early in the transperineal implant era. The coverage values shown above would, at best, be considered only marginally acceptable today. [Reprinted from *Int J Radiat Oncol Biol Phys*, vol. 40, "Timing of computed tomography-based postimplant assessment following permanent transperineal prostate brachytherapy," B. R. Prestidge, W. S. Bice, E. J. Kiefer, and J. J. Prete, pp. 1111–1115. © 1998, with permission from Elsevier.]

lations, published an historical analysis and a set of consistent dose calculation parameters for each known interstitial source type, and provided a framework for future changes in calibration and calculation methods and results. Subsequently, an update, known as TG43U1, was published which precluded the mixing of line and point source measurements and calculations, established a mechanism for determining calculation parameters from different data sets, and extended the number of sources characterized according this revised formalism (Rivard et al., 2004). TG43 and TG43U1 are covered in detail elsewhere in this monograph. It suffices to state that the publication of these two sets of recommendations had a profound impact on brachytherapy in general and that post-implant analysis should only be performed using these calculation protocols.

The Dose Evaluation Hierarchy

Table 1 shows a hierarchy of tools that are used in evaluation of post-implant dosimetry. Each will be discussed in some detail. As shown, moving down the table each tool sacrifices information for simplicity. At the top of the hierarchy are isodose curve displays. Isodose curves retain all the dose and spatial information in an implant. Regions of low and high dose are readily seen and localized. At the next level, dose-volume histogram (DVH) displays have reduced the information available by limiting the spatial information to simply being inside the structure, but have simplified the dosimetric information within the implant to a single two-dimensional (2-D) plot. Line plots or dose traces are a special case for linear type structures where spatial information can be retained in a 2-D plot. At the lowest level of the hierarchy are dosimetric quantifiers. Quantifiers are the result of distilling information from the DVH to represent a characteristic of the implant as a single value. Quantifiers are simple to use and compare, but the information from a single quantifier is really very sparse.

Keeping in mind that the purpose of post-implant evaluation is really twofold, one can see how the dose evaluation hierarchy has grown to fit nicely into its purpose. For single implant analysis, most of the time in an evaluation should be spent at the top levels of the hierarchy—the isodose displays and the DVH. Adequate dose to specific locations within the gland, like the site of positive biopsies, can be determined.

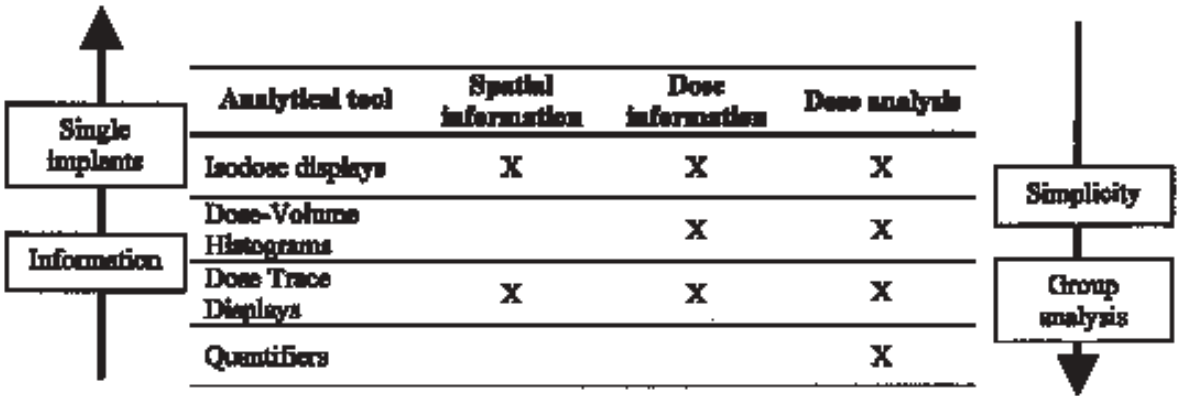

Analytical tool	Spatial information	Dose information	Dose analysis
Isodose displays	X	X	X
Dose-Volume Histograms		X	X
Dose Trace Displays	X	X	X
Quantifiers			X

Table 1. The Dose Evaluation Hierarchy

Modern treatment planning systems offer a variety of tools with which to analyze the dose from an implant. Isodose curves and surfaces contain all the spatial and dosimetric information, dose-volume histograms sacrifice the spatial information, quantifiers are an attempt to describe a characteristic of the implant with a single value. Single implants are usually analyzed at the top of the hierarchy with display isodose structures, group analysis is usually performed at the bottom of the hierarchy with quantifier evaluation.

The locations of high-dose regions in critical structures that might cause complications become apparent. Judging the sufficiency of a specific implant is best performed at the top of the hierarchy.

Evaluating the effectiveness of the implant team and the implant procedure is the subject of more than a single implant, often a great number of implants. This is too much information to glean from the tools at the top of the hierarchy; hence this sort of analysis is best performed with implant quantifiers, located at the bottom. Looking at a trend in coverage, for instance, can be falsely colored by a single bad implant. Compiling coverage quantifiers from the last 50 implants gives a pretty clear picture of how the team has progressed over time or the true effect of a procedural or equipment change.

Isodoses and Gridded Calculations

Isodose values can be shown as curves on a single slice or set of slices as shown in Figure 3 or as 3-D surfaces as shown in Figure 4. The use of tomographic image sets allows the calculation and display of the dose distribution registered to the structures of interest: the target volume and any critical structures.

Brachytherapy calculations must be performed in three dimensions. To display isodose lines or surfaces, computerized calculations are performed on a regular grid, with voxel size determined by the grid spacing. Several authors have recommended this grid spacing for brachytherapy be no larger than 2 mm (Yu et al., 1999; Nag et al., 2000). Figures 5a, 5b, and 5c show the effect of grid size selection on a simple dose distribution generated using sources and spacing commonly found in permanent brachytherapy.

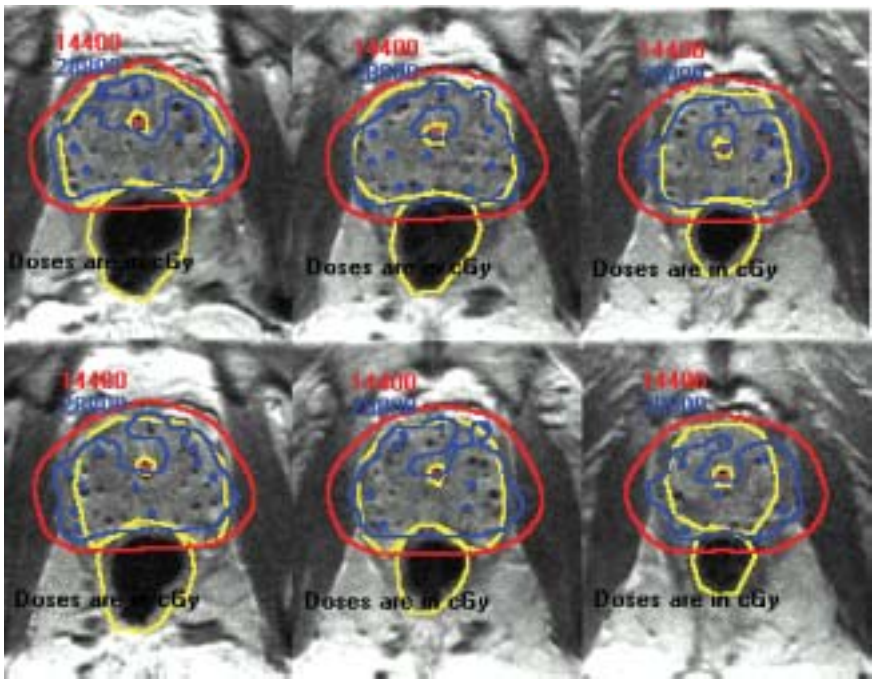

Figure 3. Isodose curves on a MR-CT fused image set.

Six consecutive, from base towards the apex, axial slices from a prostate post plan depicting delivered dose overlaid upon an MR image set in which the prostate, urethra, and rectum have been outlined. The source locations are from an axial CT data set. The image sets were fused using an iterative least squares fit to available source positions. The reference dose for this implant was 144 Gy. (Dubois, Bice, and Prestidge 2001)

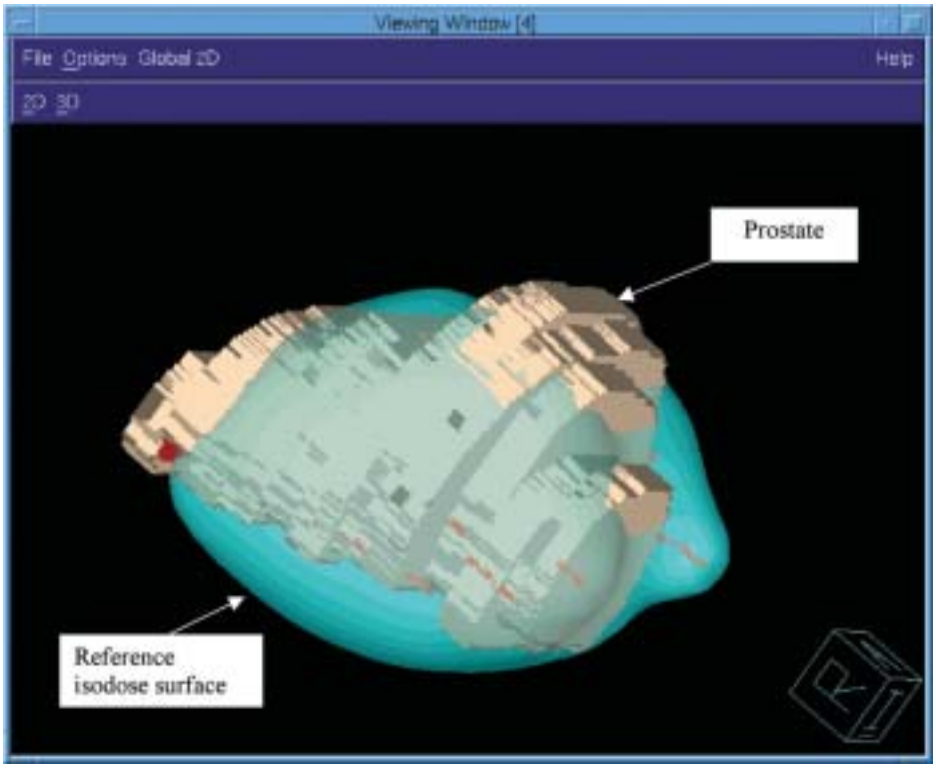

Figure 4. Three dimensional isodose surface.

Shown is the reference isodose surface on an implant where coverage of the base and anterior gland appears to be inadequate.

Dose-Volume Histograms (DVHs)

Structure- and Nonstructure-Based Histograms

Dose-volume histograms (DVHs) are used in brachytherapy to display graphical representations of radiation dose to structures. With the exception that the dose values calculated pertain to volume elements that lie somewhere within the structure for which the calculation is performed, spatial information is lost in the DVH. In the DVH, volume is usually the dependent variable and is plotted against dose, usually the independent variable. When convenient, percent volume may be shown as opposed to volume. The DVH for the prostate gland for an implant is shown in Figure 6. The low-dose region at the anterior base can be seen as a drop off of the curve below 100% of the volume at a dose less than the prescription or reference dose (vertical line). The specific location of high-dose and low-dose regions within the gland is not discernible in the DVH.

Less occasionally, the DVH may be presented as nonstructure based. This is a DVH of the entire calculation volume. Whereas this presentation was used extensively prior to being able to determine target locations in the image sets, it is rarely used now. Analysis is predominately restricted to structure-based DVH, even if there are gross uncertainties in the precise location of the structure.

Integral Dose-Volume Histograms (IDVHs)

Figure 6 shows an integral or cumulative DVH (IDVH). The ordinate for each point on the curve represents the volume or percent of volume of the structure that achieved greater than or equal to the dose on

Figure 5. Effect of grid size on isodose calculation and display.

Figure 5a. Slice 0 of the RTOG prostate phantom calculated with a 4-mm grid size. This is a common default resolution for external beam radiotherapy planning systems.

Figure 5b. The same slice but with a 2-mm grid size.

Figure 5c. The same slice with a 1-mm grid size. Note the marginal improvement over the 2-mm calculation grid.

This figure illustrates the effect that grid size has on isodose calculation and display. A 2-millimeter grid size has been considered an adequate compromise between speed and accuracy and is recommended as the largest grid appropriate for prostate brachytherapy. Most modern treatment planning systems easily achieve rapid calculation times even with grid sizes as small as 0.5 mm.

the abscissa. For example in the DVH shown, 50% of the prostate received at least 180 Gy. The IDVH is by far the most prevalent DVH display; practitioners commonly refer to the integral DVH as simply the DVH, reserving the terms integral or cumulative only when required to differentiate between other forms of dose-volume display.

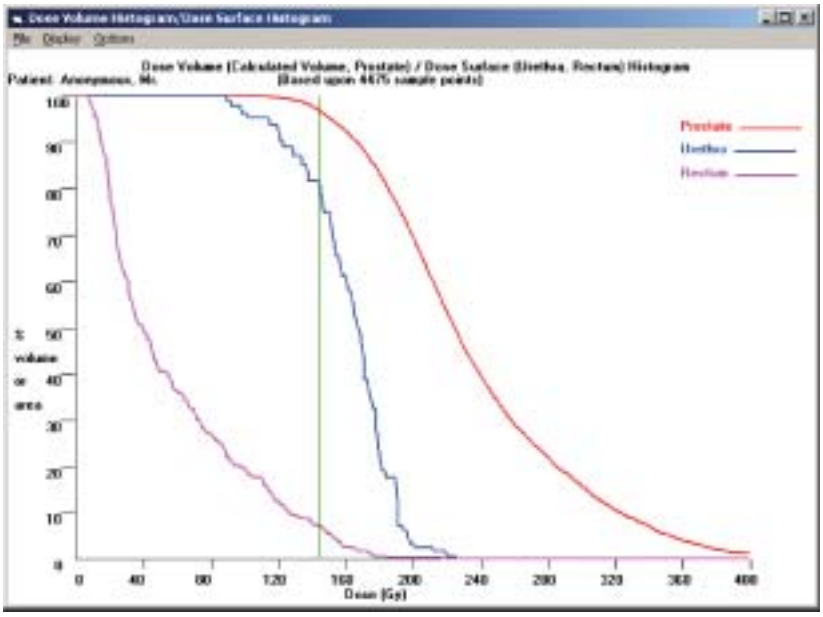

Figure 6. Dose-volume histogram.

This is the dose-volume histogram, or integral dose-volume histogram, for the prostate gland following an iodine monotherapy implant. Percent volume of the gland that achieved that dose or greater is plotted against the dose in Gy. The reference dose of 144 Gy is shown as a vertical line. V_{100} for the implant was 97%. Also shown are the dose-surface histograms for the urethra and the rectum.

Differential Dose-Volume Histograms (DDVHs)

One alternative form of the DVH is the differential DVH (DDVH). The DDVH for the prostate IDVH of Figure 6 is shown in Figure 7. In the DDVH, each point on the curve represents the volume or percent of volume of the structure that received the dose value encompassed by the bin values, neither more nor less. The DDVH in Figure 7, for example, shows that 0.32 cm^3 of prostate volume received a dose between 179 and 180 Gy (the bin range for the 179.5 Gy bin). Because the plot was normalized, this information is obtained from the inset box.

Also shown in this figure is the DDVH for the entire calculation volume. Without a structure in the image set, this would have been all that was available to the early practitioners of brachytherapy dosimetry. Note the large volumes in the calculation volume DDVH. The low doses overwhelm the high-dose regions, largely due to the inverse square law. Hence there exists the need for normalizing this plot to the largest value for each curve. How frustrating it must have been for these early practitioners to realize that the information of interest, the information about the target region, is in the calculation volume DDVH, but the structure of the curve is hidden by displaying the low-dose regions.

Natural Dose-Volume Histograms (NDVHs)

A third type of DVH is used in brachytherapy, particularly in situations where the target volume is unknown or not displayed in the image set. The natural DVH (NDVH) was developed by Anderson to remove the inverse square law effect from the DDVH (Anderson 1986). Instead of graphing simple volume in the DDVH, the NDVH plots volume divided by dose raised to the -3/2 power against dose. This has the very desirable effect of enhancing the higher-dose regions of the dose display while depressing the lower-dose regions. In the simple DDVH the graph is overwhelmed by the larger volume of the low-dose

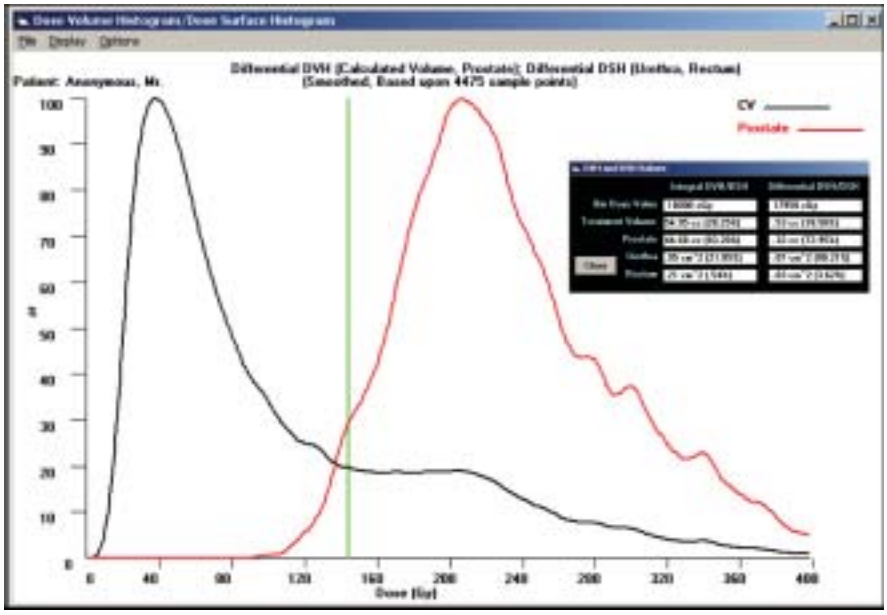

Figure 7. Differential dose-volume histogram.

These are the differential dose-volume histograms, the prostate and the entire calculation volume, for the same implant as shown in Figure 6. Each point on the curve represents the volume, or percent volume, that received the dose indicated by the 1 Gy bin. The displays have been normalized due to large differences in the volumes. The inset shows actual values. See the text.

regions, obscuring the information where the doses are the greatest, usually within the target structure. Figure 8 illustrates this effect and how the NDVH provides a remedy. Note the lack of visible information at doses greater than the reference dose (the vertical line) in Figure 7. Figure 8 shows the NDVH for both the calculation grid and the prostate gland. Note the similarity at doses greater than the reference dose, the major discrepancy being dose regions greater than the reference dose but outside the gland. Anderson and other investigators used the NDVH to see dose structure at high-dose regions in and around the implant, presumably where the target volume is located, to evaluate the quality of implants, even though the target volume is not seen in the image set. Some commercial planning systems have applied the NDVH approach to defined anatomic structures or target volumes (Moerland et al., 2000).

Dose-Surface Histograms (DSHs)

Dose-surface histograms (DSHs) can also be used to portray the dose on the surface of structure where volumetric dose may be less meaningful. An example of this is the rectum, where dose to the rectal wall is probably more important than dose to anything within the rectum. DSHs plot surface area or percent surface area on the ordinate. As with the DVH, a differential DSH can be developed as well as a natural DSH, although the utility of the latter is not entirely apparent.

Dose Traces

The dose trace or line plot is an appropriate graphical depiction of dose for small linear structures. For prostate brachytherapy, this display has been used as a tool for analyzing the dose to the urethra and the neurovascular bundles. In HDR brachytherapy, comparative displays of measured versus calculated dose at points within the urethra have been the subject of dose traces (Anagnostopoulos et al., 2003). A urethral dose trace for the implant shown in Figure 6 is shown in Figure 9.

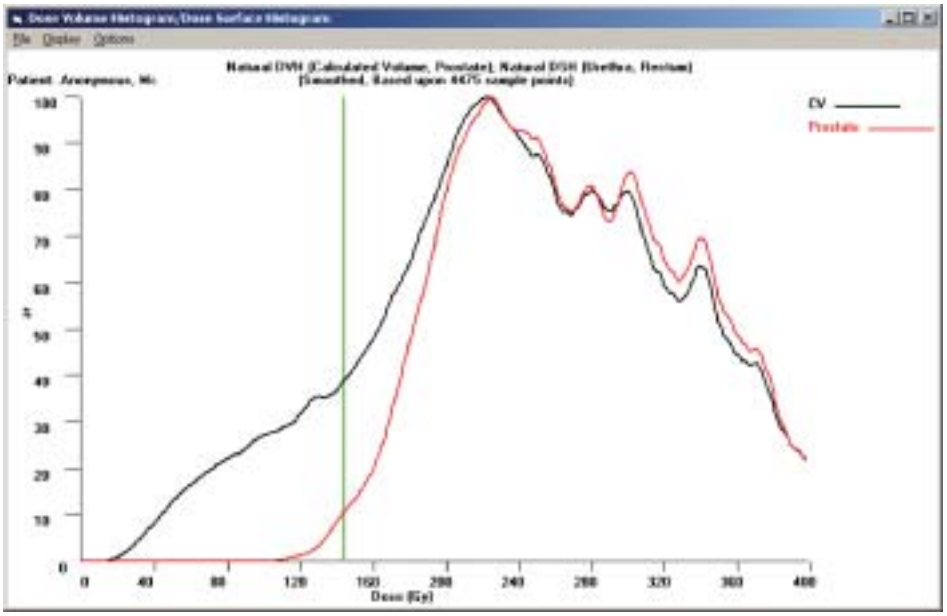

Figure 8. The natural dose-volume histogram.

The natural dose-volume histogram removes the effect of lower doses having larger volumes because of the inverse square law. Shown are the NDVH for the entire calculation volume and the prostate volume as in Figure 7. The similarity of the curves in the regions above the reference dose indicate that the NDVH can be used to tease out information about the target doses when there is no target visible in the image set. This relies of course upon the assumption that the high dose regions were delivered to the target.

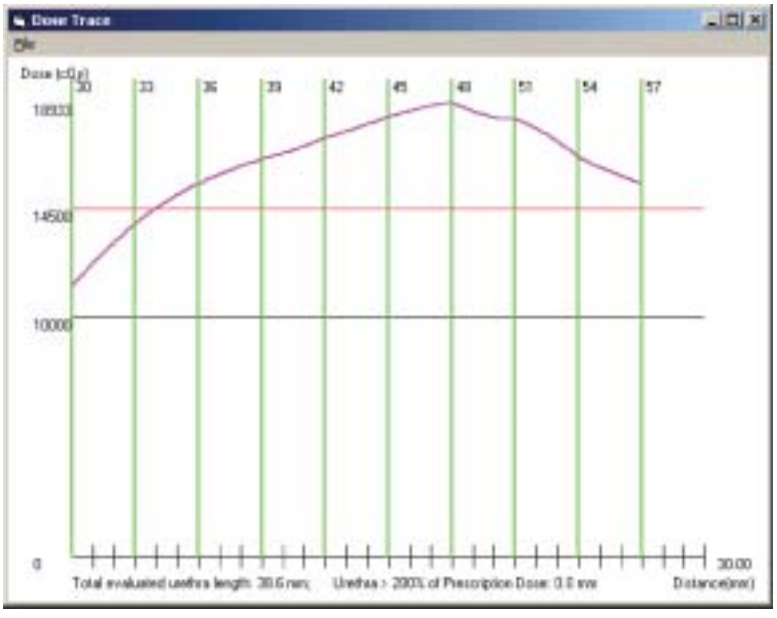

Figure 9. Urethral dose trace.

This is a dose trace along the center of the urethra for the implant of Figure 6. The distance is measured along the urethra from base to apex slices. Only the first 2.7 cm of the length of the urethra is shown. Slice positions are indicated at the top of the vertical lines. The maximum dose of 189 Gy can be seen to occur at slice position 48 (1.8 cm from the base).

DVH Sampling

DVHs are created by sampling the target volume, calculating the dose to sample point (representing a sample volume), and binning the result. The DVH created from a grid calculation is an example of sampling at regular intervals. The optimal sampling technique and the uncertainty due to sampling of the target volume have been the matter of some debate (Lu and Chin 1993; Niemierko and Goitein 1994; Karouzakis et al., 2002). This uncertainty can best be seen in the DDVH. Figures 10a through 10e are examples of DDVH created by regular grid sampling, random sampling with varying numbers of samples, and the sampling noise removed from regular grid sampling by convolving the result with a simple box filter (moving averages in the financial world). As can be seen, generating a less noisy DDVH is possible with any of these methods, but the uncertainty with regard to the result, particularly for brachytherapy DVH, has yet to be studied and quantified.

Quantifiers

Dosimetric quantifiers are used to further distill the information from the DVH down to a single value that describes some aspect of the implant. Like the DVH from which they are derived, quantifiers may be structure based or nonstructure based. Several quantifiers have both forms: for instance, the nonstructure-based dose non-uniformity ratio (DNR) (Saw and Suntharalingam 1991) and V_{150} that is structure based. Both are calculated similarly, the volume encompassed by the surface described by 150% of the reference dose divided by the volume of the surface encompassed by the surface described by the reference dose (the DNR) or else divided by the volume of the target (V_{150}). Quantifiers are used to describe certain attributes of the implant. These can be classified as describing either structure coverage or dose uniformity.

Coverage Quantifiers

Coverage quantifiers, for obvious reasons, are usually restricted to structure-based DVH analysis. A possible exception is the use of matched peripheral dose (MPD), which may be derived from a non-structure based DVH. The MPD, originally developed as a design tool, is the dose that encompasses the same volume as the volume of the target. Although MPD does not require locating the target in the image set, as a coverage quantifier this really is a fatal flaw, indicating nothing about the relative location between the dose distribution and the target. MPD is rarely used for post-implant evaluation.

Coverage quantifiers can be grouped according to the Volume quantifiers (V) and the Dose quantifiers (D). V quantifiers describe the volume of the structure that receives at least a certain dose. Both the volume and the dose may be stated as a percentage, the first as a percentage of the target volume, the second as a percentage of the reference dose. The V quantifier is subscripted to indicate the dose, or percentage of dose, to which the quantifier refers. For instance, V_{150} refers to the volume, or percentage of the volume, that receives at least 150% of the reference dose. Note that V_{150} could also refer to the volume, or percentage of the volume, which receives 150 Gy, or 150 cGy, or some other expression of a dose of 150 of some unit. In this regard, the nomenclature is indistinct. The majority of the time, both the volume and the dose are expressed as percentages, allowing comparison between implants that were performed on different volume targets and which had different reference doses—even different isotopes.

Common usage has modified, to a degree, the format of the V quantifiers. Used to describe coverage of the target, a V is almost always used, but in describing dose to critical structures, the V may be replaced with a letter pertaining to the critical structure. For instance R_{100} may refer to the volume, or percent of volume, of the rectum which receives 100% of the reference dose or greater; U_{200} the volume, or percent of volume, of the urethra which receives 200% of the reference dose or greater.

Figure 10. Sampling errors in the dose-volume histogram.

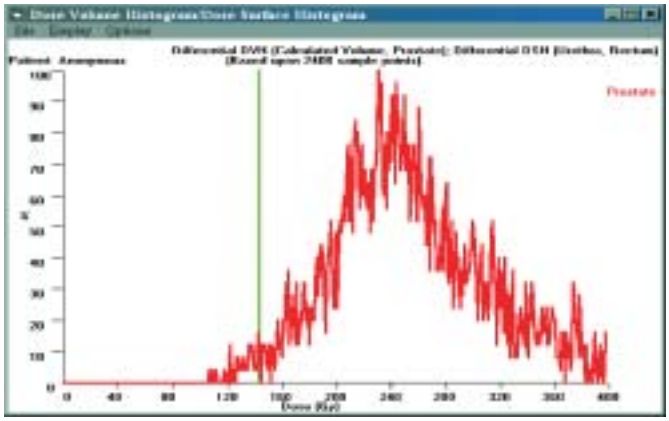

Figure 10a. The DDVH calculated directly from a 2-mm grid.

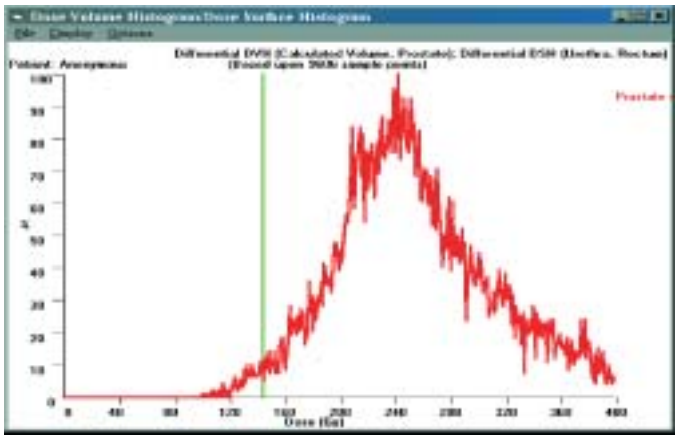

Figure 10b. The DDVH calculated directly from a 1-mm grid.

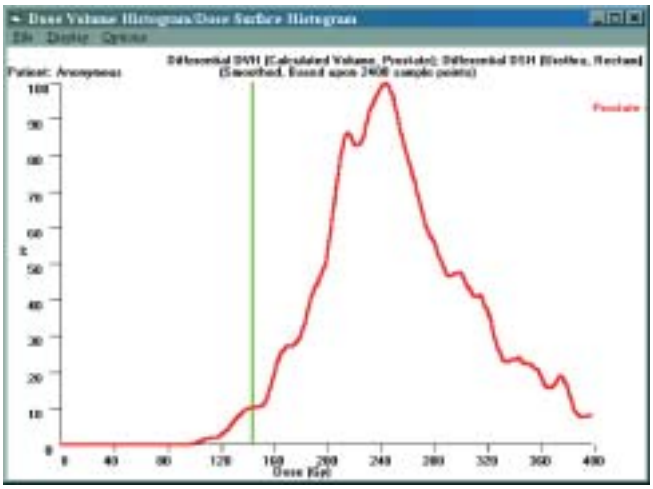

Figure 10c. The DDVH calculated from a 2-mm grid with a simple box filter smoothing routine.

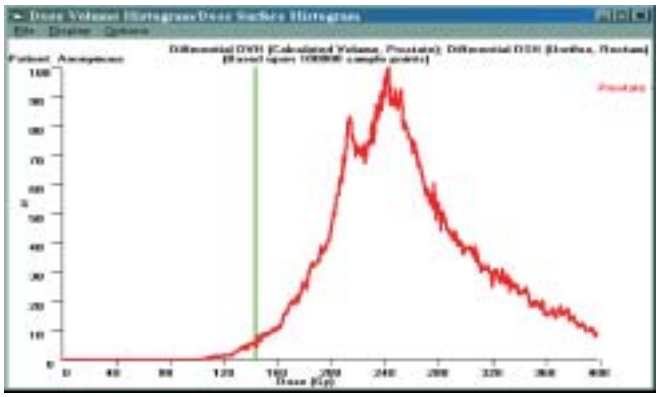

Figure 10d. The DDVH calculated from 100,000 random samples.

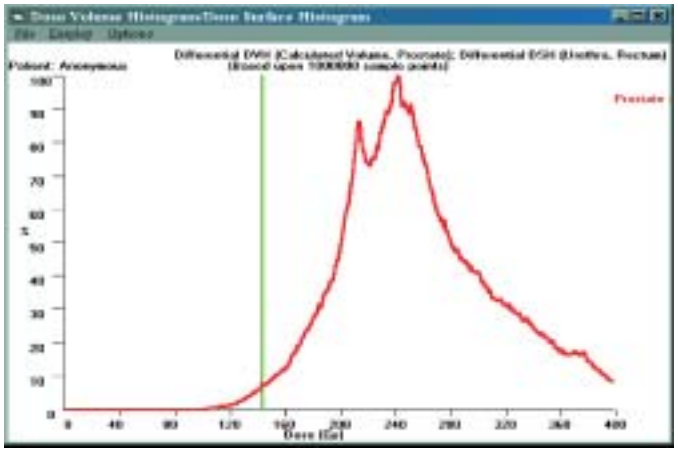

Figure 10e. The DDVH calculated from 1,000,000 random samples.

This series of differential dose-volume histograms shows the noise inherent in creating the DDVH. Most treatment-planning systems that show the DDVH use some sort of smoothing routine to generate a less noisy plot. There is some difference between Figures 10c (under sampling and smoothing) and 10e (heavily sampled), but the clinical significance is probably marginal.

It may also be misleading or inappropriate to normalize the value of the volume in presenting the quantifier. Stating a rectal dose quantifier like R_{100}, in terms of a percentage of the rectal volume may portray no useful information. Rectal complications are most likely related to the volume of the rectum that receives a certain dose, not a percentage of the rectum that received that dose. The added complication of using an indeterminate length to describe the rectum is also thus avoided by quoting the value of the volumetric quantifier in volume rather than as a percentage, 3.8 cm^3 versus 20%, for example.

D quantifiers describe the dose at which a given volume of the target receives that dose or greater. Like V quantifiers, D quantifiers are subscripted, this time with the volume rather than the dose. Again the value of the quantifier and the subscript may be normalized or not and the distinction is not always clear. D_{90} for instance most commonly means the dose, or percentage of dose, that encompasses 90% of the target. It may also pertain to 90 cm^3 or 90 mm^3 or 90 of some other unit of volume. Unlike the V quantifiers, D quantifiers usually normalize the volume but rarely normalize the dose. This allows comparison between targets of different volume, but not between implants with different reference doses. Occasionally the need

does exist. For example, when performing comparisons between implants performed with different isotopes or when including implants performed as monotherapy and implants performed as boost therapy in the same data set, different reference doses are used. In these cases the D quantifier must be normalized to the percentage of each implant reference dose.

Because the V quantifiers and the D quantifiers both describe coverage of the target, it would be surprising they were independent of each other. Figure 11 is a graph of this relationship between implants performed at a single institution. For the implant design and delivery methods used at this institution, V_{100} = 87% was equivalent to D_{90} = 100% of the reference dose. This held true for both iodine implants with a reference dose of 145 Gy and palladium implants with a reference dose of 125 Gy (115 Gy, prior to 2000). This relationship is probably strongly related to the practices adhered to by a specific implant team, and is not therefore generally applicable.

Uniformity Quantifiers

The doses in brachytherapy are, by nature, inhomogeneous. Nevertheless ignoring the size of the high-dose regions would be folly. Excess dose that does not contribute to curing the disease enhances the risk of complications. The question of wasted dose in prostate cancer has been studied by Ling resulting in the conclusion that doses in excess of 125% of the prescription dose probably do not contribute to curing the disease (Ling et al., 1994). Inhomogeneity quantifiers fall into two categories: those that quantify the inhomogeneous nature of the dose and those that simply quantify the size of the high-dose regions. The best example of a quantifier that describes the homogeneity of an implant is the full width at half maximum (FWHM) of the DDVH; the smaller this value, the more homogeneous the implant. V_{150} is the most common example of a quantifier that describes the size of the high-dose regions in the implant. As described previously, this is the percentage volume of the gland that receives greater than 150% of the reference dose.

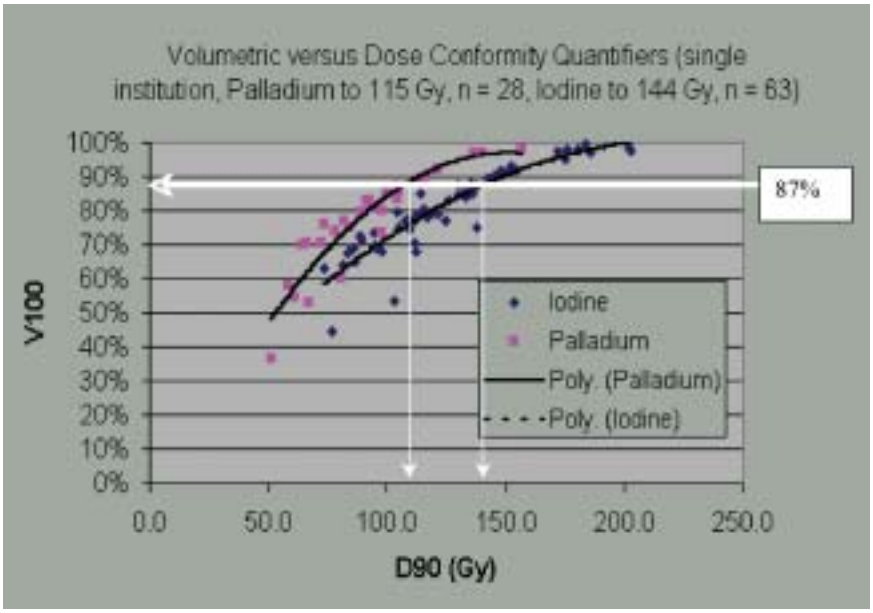

Figure 11. The relationship between V_{100} and D_{90} at a single institution.

V_{100} and D_{90} both describe coverage of the gland and it is not surprising that they correlate. For this institution, a V_{100} of 87% may be interpreted as about the same coverage as a D_{90} equal to the reference dose. This was true for both iodine and palladium implants.

Uniformity and the size of the high-dose region are not necessarily related. This is shown in Figure 12, where the DDVH for two implants with similar V_{150} have dramatically different uniformity as measured by the FWHM DDVH. It should be noted that the value of V_{150} is only meaningful as a quantifier of true dose uniformity if used when comparing implants with the same coverage by the reference dose, V_{100}, or if V_{150} is normalized to V_{100}. Despite this, V_{150} is more commonly used than the dose homogeneity index (DHI) because complication rates are thought to be much more likely due to excessive dose rather than non-uniformity of the dose distribution. The DHI is equal to the [V(TDR) – V(HDR)]/V(TDR), where V(TDR) is the volume covered by the target dose-rate and V(HDR) is the high dose-rate volume—usually the volume covered by 1.5 times the target dose-rate (Wu, Ulin, and Sternick 1988). Because V_{150} is the percentage of the target volume that has a dose greater than 150% of the reference dose, one might assume that V_{150} is equal to (1 – DHI). This is not, in general, true for two reasons. First, the denominator for V_{150} is the entire gland volume, not just the volume covered by the reference dose. Second, the DHI, originally developed for iridium implants, is still usually considered a nonstructure-based quantifier.

Critical Structure Dosimetry

Dosimetry for critical structures varies according to the structure type. In an effort to calculate doses that will correlate to complications that arise from the dose delivered, most brachytherapists have strived to tailor the dose calculation, display, and evaluation to the form of the structure. Consider the possible critical structures in prostate brachytherapy. The bladder and rectum might be more amenable to DSH analysis; the urethra and neurovascular bundles, line dosimetry; the penile bulb, a DVH; the bladder neck; a point calculation. Efforts have been made to standardize critical structure dosimetry and reporting, but with much less success than in standardizing target dosimetry (Yu et al., 1999; Nag et al., 2000, 2002). For instance, the dose to the rectum has been characterized by different investigators as a DVH, an annular DVH, a DSH, a dose trace, and as a single point value. Urethra doses have been characterized in terms of length, area, and volume. The West Virginia group found that within some limitations all of these methods were viable and comparable as analysis tools for post implant evaluation (Merrick et al., 1999a; Butler et al., 2000a). An excellent investigation of the optimal replication of rectal surface dose measurements was performed by Hilts et al. (Hilts, Spadinger, and Keyes 2002). Looking at length of rectum, average anterior dose, and DVH of the rectum, they found that the DVH of the anterior half of the rectum was the optimal alternative to DSHs.

Dosimetric Uncertainty

The vast majority of our credible knowledge pertaining to post-implant evaluation of prostate implants comes from CT imaging. As previously noted, it is very difficult to precisely delineate glandular borders on CT. The effect on post-implant dosimetric quantifiers has been reported by various authors, but without consensus. Contouring recommendations have been developed by various groups (McLaughlin et al., 2002; Crook et al., 2002).

Figure 1 showed the results in the coverage quantifiers for expansion and contraction in 2 mm increments of the prostatic contours for a series of implants as shown in Figure 13. No expansion was performed in the posterior direction as the extent of the gland is more easily visualized due to the presence of the rectal wall. The effect of this expansion and contraction scheme on 50 ^{125}I implants is graphed for V_{100} in Figure 1a and D_{90} in Figure 1b. An analysis of 30 palladium implants gave very similar results, as do other expansion methods used to perform the same analysis. As can be seen, drawing the gland too large makes the coverage quantifiers smaller, drawing the gland too small makes the coverage quantifiers larger, but to a lesser extent. One would conclude that erring in the smaller direction would likely be more accurate. One practitioner uses the pre-implant ultrasound volume, without edema, to overlay and contour the post-

Figure 12. The difference between V_{150} and uniformity.

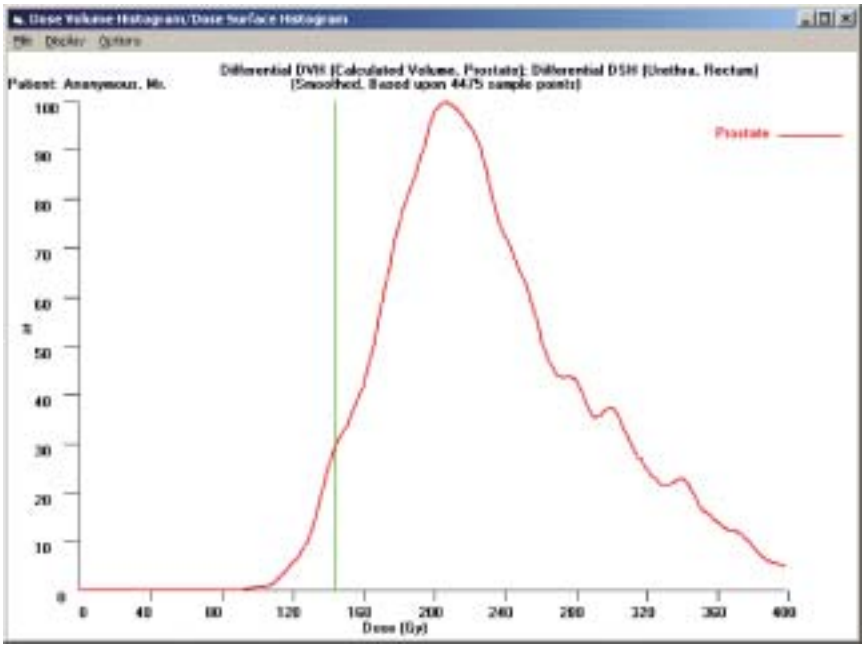

Figure 12a. The DDVH for an implant with V_{150} = 55% and FWHM = 96 Gy.

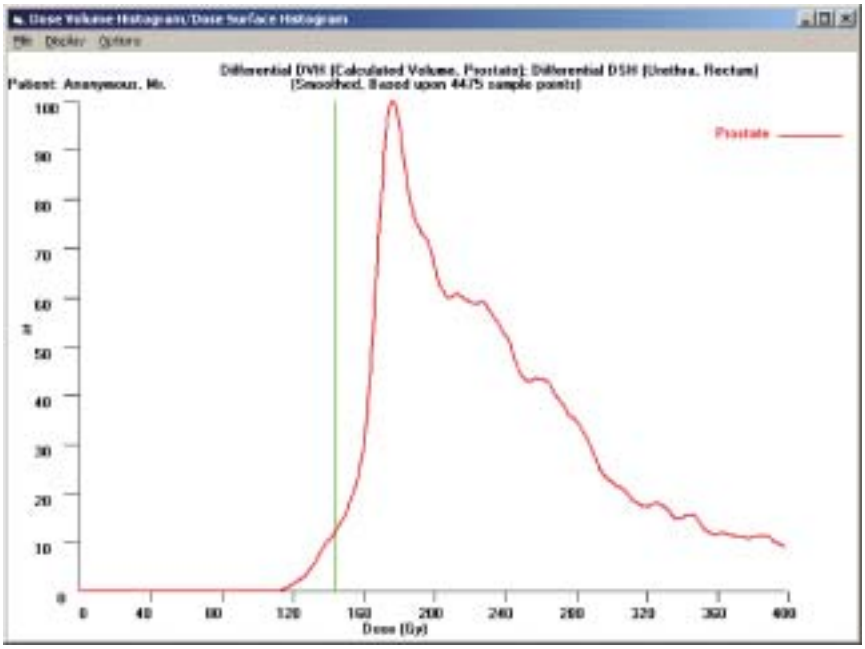

Figure 12.b. The DDVH for an implant with V_{150} = 55% and FWHM = 77 Gy .

Although commonly used as such, V_{150} is not really a measure of implant uniformity. The implant in Figure 12b. is more uniform than that in 12a. (FWHM of 77 Gy versus 96 Gy), but both have a V_{150} of 55%. The relationship between V_{150} and FWHM is dependent upon target volume, source strength, and implant design.

Figure 13. Expansion and contraction of the glandular volume.

One possible method of expansion and contraction of prostatic contours from post-implant CT scans is shown here. The gland was grown or contracted in 2-mm increments about the center of mass, except in the posterior direction, where the glandular borders are more visible than in the other directions. The analysis was performed in order to estimate the effects of uncertainty in drawing the glandular borders. The results are shown in Figures 1a. and 1b.

operative, edematous gland on CT. While this almost certainly overestimates the prostatic coverage, it has the advantage of consistency, being based on an imaging modality in which the glandular borders are readily visible, and the advantage of erring in the too-small direction, the direction of smaller error (Badiozamani et al. 1999; Smith et al., 2003).

Finding and contouring the location and extent of critical structures on a CT can also present difficulties. The urethra is best visualized following catheterization, not necessarily a problem if the post implant imaging is performed immediately following the procedure, but at significant discomfort to the patient if performed at a later time. A retrograde urethrogram, although less invasive, is inadequate due to the inability of the dye to cross the urogenital diaphragm. Neurovascular bundles (NVB) may or may not be critical structures for retention of potency; the uncertainty is probably due in part to the inability to visualize them on CT. Work has been performed recently using MRI to localize the NVB in prostate brachytherapy (McLaughlin et al., 2005). The rectal wall, penile bulb, and bladder are usually of sufficiently dissimilar contrast when compared to adjacent structures to be adequately visualized in CT image sets.

Dynamic Dosimetry

While prostate brachytherapy offers a unique opportunity to evaluate the dose being delivered from sources that are visible alongside the target and critical structures, it should be remembered that the image set still only provides a single snapshot of the dose delivered over the life of the implant. The resolution of post-implant edema, seed migration, and anatomical changes can all occur while the radiation dose is being delivered. Roy and Ling have performed extensive radiobiological analyses for iodine prostate brachytherapy, calculating the effective life of an iodine implant to be about 275 days (Roy et al., 1993a; Ling et al., 1994). During this time the relative change between source locations and the structures of interest has not been rigorously studied. Models which characterize edematous changes have been developed which portray the effect of these changes in dosimetric coverage of the gland, but very little has been done to quantify the resolution of edema on the dose to critical structures. Waterman and Dicker (1999, 2000) did show a continuous, exponential increase in rectal dose R_{10} and in urethral dose as edema resolved.

Most seed loss probably occurs within the first week following the implant. The most common mechanism for this is likely migration through the bladder or urethra wall and subsequent elimination with the urine. Occasionally seeds work their way into the periprostatic arteriovenous complexes and can later be found in the lung or heart tissues. The migration of seeds is less for stranded seeds than for loose seeds. This sort of seed loss is thought to have little effect on the dose delivered in permanent brachytherapy, but temporal studies have yet to be performed which illustrate this (Merrick et al., 2000a; Fuller, Koziol, and Feng 2004).

Advanced Techniques

Subglandular Analysis

Several techniques have been used to perform subglandular targeting of dose. One institution implants only the peripheral zone of the prostate, based upon extensive biopsy data that shows the likelihood of cancer occurring elsewhere within the gland to be extremely small. These implants are performed under MRI-guidance so that the peripheral zone may be imaged (D'Amico et al., 2000; Kooy et al., 2000). Other institutions have used MR spectroscopy or ^{111}In imaging (see Figure 14) to locate most likely foci of disease within the gland (Ellis, Kim, and Foor 2004). These brachytherapists still target the whole gland but increase the dose locally at the cancer sites. Whether the intent is to reduce complications or to boost the dose to sites of active disease, there is an increased challenge to post-implant evaluation. First, imaging of the subglandular target must be performed with a modality in which this target can be seen. If imaging using this modality is performed pre-implant only, registration of the pre-implant image set to the post-implant image set is plagued by changes not only in the shape and location of the edematous gland, but also possibly uncorrelated changes in the subglandular target volume. MRI and nuclear medicine imaging are inadequate for seed localization, which implies the need for a second imaging modality, along with the inherent problems of fusion methods and added cost.

Creation of the DVH for a structure removes all the spatial information with regard to the distribution of dose within the target. Sector analysis was developed to retain some of this information while still maintaining the simplicity of DVH and quantifier comparison. In this technique the gland is divided into 12 sectors, 4 each at the base, midgland, and apex, as shown in Figure 15. A DVH is then created for each sector, each with a corresponding set of quantifiers. Sector analysis is particularly useful for analyzing a series of implants. Trends in implant technique can be teased from a very large data set (Bice, Prestidge, and Sarosdy 2001),

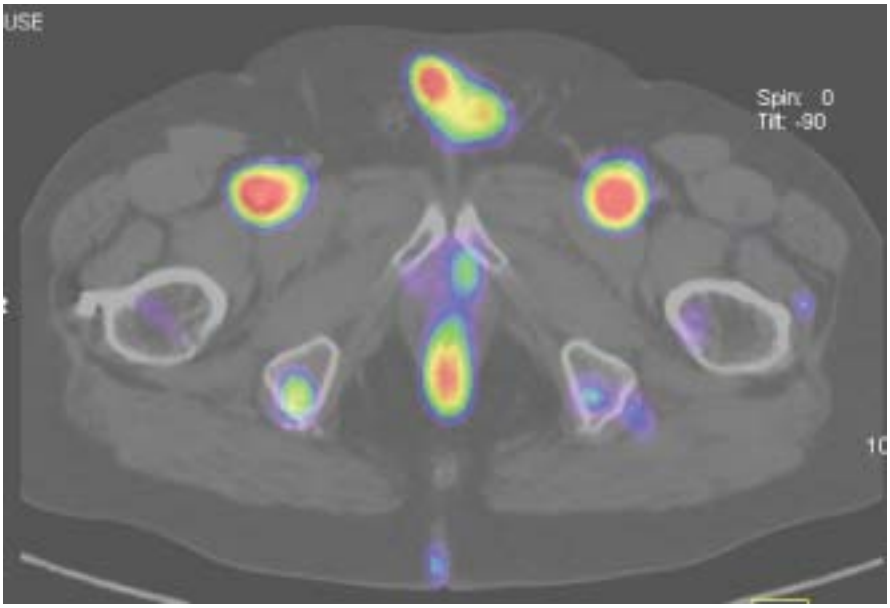

Figure 14. SPECT image using ^{111}In.

Partial volume brachytherapy boosts are possible using SPECT imaging or magnetic resonance spectroscopy. This image was taken 5 days following the injection of ^{111}In, showing uptake on the left side of the gland in the peripheral zone. This presents a unique challenge with regard to post-implant dosimetry; target subvolumes have not been studied with regard to what doses are appropriate or achievable. Localization of the subvolume almost certainly requires the fusion of two or more image sets, some acquired before the implant, some after.

Sensitivity Analysis

The inability of the brachytherapist to position the sources precisely as planned has been of concern since the beginning of post-implant planning and analysis (Roberson et al., 1997). Several investigators have used source displacement analysis to model the effect of the source misplacement and/or local migration on the quality of the implant (Roberson et al., 1997; Wuu et al., 2000; Beaulieu et al., 2004). These techniques rely on post-implant evaluation to develop a model for source displacement and then apply this model to either pre-implant design or to temporal analysis over the life of the implant. Table 2 shows the utility of displacement analysis for determining the sensitivity of an implant design to misplacement of the sources. In this particular table the sensitivity of glandular coverage to source displacement is quantified as the average and standard deviation of D_{90} based upon 50 iterations of source displacement using randomly distributed values of displacement. Practitioners often refer to this sensitivity as a measure of design robustness.

Correlation of Clinical Results to Post-Implant Dosimetry

In citing clinical results for PPB, note the difficulties associated with conducting and publishing results for this disease. Despite attempts to automate and standardize the methods used to design and perform the implant, dosimetric results are still largely dependent upon the skill of the practitioner—a skill which changes with the acquisition of experience. Evaluation tools are not truly standardized, nor are analysis and reporting techniques. Prostate cancer is an extremely indolent disease. With regard to cure, databases are not really mature until the 10- or 15-year mark. Complications usually occur within the first 1 or 2

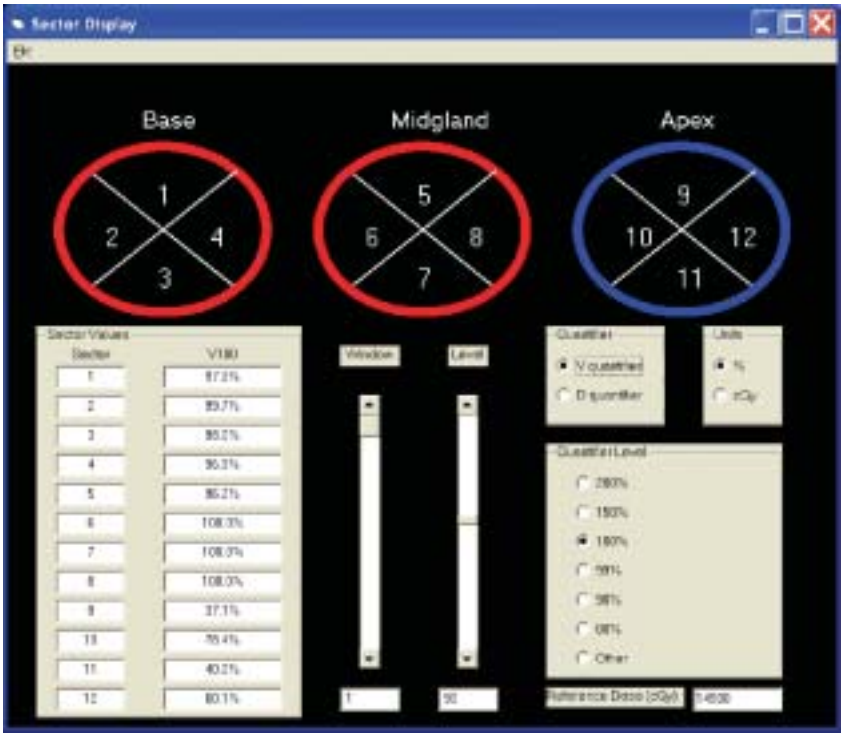

Figure 15. Sector analysis.

Sector analysis allows retention of some of the spatial information dose to certain regions of the gland while affording the advantages of dose-volume histogram and quantifier analysis. Shown above is the sector results for an implant that was adequately covered well at the base (sectors 1–4) and the midgland (sectors 5–8), but the coverage at the apex was questionable. While the practitioner would probably be able to glean this sort of information from a set of isodose curves, such an approach has the disadvantage of being difficult to quantify and would be inappropriate for analysis of a large database.

Table 2. Displacement Analysis Results

Design	Number of Sources	Source Strength (U)	Total Strength (U)	V100 Design (Displaced) %	V150 Design (Displaced) %	D90 Design (Displaced) Gy
Design #1	66	0.432	28.5	99.5 (90.4 ± 3.5)	65.2 (37.6 ± 8.5)	186 (147 ± 6)
Design #2	45	0.635	28.6	99.4 (87.6 ± 4.1)	68.4 (44.6 ± 9.1)	183 (139 ± 9)

This is an example of source displacement analysis. It can be used for pre-planning, as was done here, or post-planning. This table compares two types of implant design for iodine monotherapy on a 22.2 cm^3 gland, one high activity, one low activity, but both with the same total source strength. Each design was submitted to 20 trials of random displacement (Gaussian displacement, isotropic, mean of 0.0 mm, one standard deviation of 5.0 mm). The ability of Design #1 to better withstand the rigors of displacement would make us tend to label it as the more robust of the two.

years following the implant, but statistical significance is often difficult to achieve simply because serious complications from the procedure are infrequent. Studies characterizing complication rates often entail following large patient populations for a significant period of time.

Cures

Early studies describing adequate prostate brachytherapy implants centered on coverage of the target volume, but lacked any correlation with clinical outcomes (Willins and Wallner 1997). The first published dose response study for permanent prostate brachytherapy was based on the post-implant evaluation of 134 early-stage prostate cancer patients at Mt. Sinai Hospital in New York (Stock et al., 1998) who had undergone iodine implants. The analysis was performed by correlating post-implant, CT-image generated D_{90} for these patients to biochemical control of the disease: the decrease of prostate specific antigen (PSA) levels following the implant. Stock found a statistically significant ($p=0.02$) difference in control rates between patients that had a post-implant D_{90} of greater that 140 Gy and those that had a D_{90} of less than 140 Gy. The first group had an actuarial control rate of 85% at 6 years while those patients in the second group had a control rate of 45%.

These results were later confirmed by Potters et al. (2001), and extended to palladium monotherapy implants with a cutoff D_{90} of 125 Gy. As was shown in Figure 9, D_{90} of 145 Gy for iodine monotherapy and D_{90} of 125 Gy for palladium monotherapy both correspond, for the institution shown, a V_{100} of 87%.

Complications

The most common rectal complication from prostate brachytherapy is proctitis, resulting in bleeding. Many authors have successfully correlated rectal complications with post-implant dose to the rectum (Han and Wallner 2001; Snyder et al., 2001; Merrick and Butler 2004). But as previously mentioned, the nonstandardization of determining the rectal target volume has made comparison of results difficult. The earliest rectal dose post-implant analysis was published by Wallner in an analysis of 45 iodine monotherapy patients (Wallner et al. 1995). The conclusion of this work was that doses to significant portions of the rectum, when converted to TG43 calculation formalism, be limited to 90 Gy. Merrick, calculating doses to the length and surface area of the anterior mucosal surface, determining mean, median, and maximum values showed that a more reasonable estimate of the allowable dose to 1 cm length of the rectum should be 100% of the reference dose, 145 Gy for iodine, 125 Gy for palladium. The maximum dose should be limited to 120% of the reference dose. This study included 45 patients (Merrick et al., 1999a). Snyder et al. (2001), in a 212-patient study, quantified results from an annular DVH described by the outer rectal wall and the inner, mucosal surface of the rectum and showed that keeping all but 1.3 cm^3 of the resultant volume below the reference dose of 160 Gy resulted in less than 5% chance of Grade 2 proctitis. These results were tabulated and are graphed in Figure 16 as an example of a complication DVH; dose-volumes to the right of the line result in 5% chance of Grade 2 proctitis. Similar findings were published by Han and Wallner (2001) in studying results from 160 patients using both surface area and a DVH generated simply from the outer rectal wall. This study, using the reference dose as a cutoff found significant differences between bleeders and nonbleeders at 3 cm^2 versus 7 cm^2 and at 0.6 cm^3 versus 2.5 cm^3.

Similar analyses of urethral complications have achieved less success. Urethral complications consist of both irritative and obstructive symptoms with the latter being more morbid. Wallner recommended keeping the dose to the urethra below 360 Gy (TG43) (Wallner et al., 1995). By 1998 Desai et al. (1998) had been able to correlate an increase in urinary symptoms with dose to gland and dose to the urethra, but made no specific recommendations. Stock and Stone (2002) found a correlation between excessive prostate D_{90} values and urethral complications and recommended keeping D_{90} below 180 Gy for iodine monotherapy. Excessive doses, greater than the reference dose, to the membranous urethra were found to result in

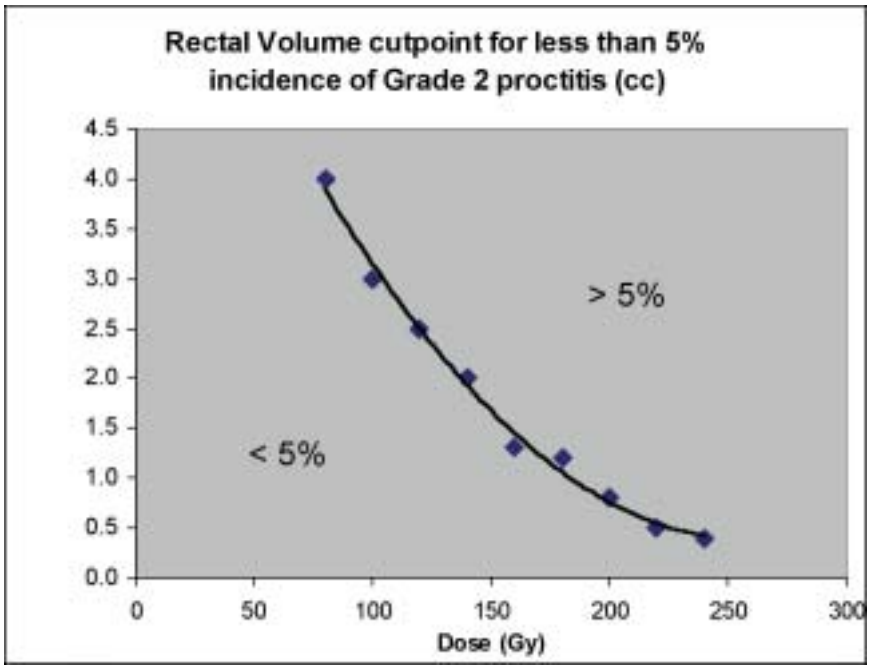

Figure 16. Dose-volume analysis of rectal complications.

Snyder et al. (2001) analyzed Grade II rectal proctitis rates from iodine monotherapy patients and tabulated the results. The analysis was unique in that, by holding the probability of occurrence constant, the authors were able to determine the probability of occurrence over a range of dose-volume values. The figure above is a portrayal of these data in the form of a complication DVH. If the rectal DVH were calculated in the same fashion as in the reference and plotted on this graph, a line that crossed over or laid to the right of the curve shown would presumably indicate a 5% chance of Grade 2 proctitis.

urethral obstruction in a retrospective, matched-patient study by Merrick et al. (2002). This same study also was able to correlate D_{90} and V_{150} to urethral obstruction.

Multiple authors have attempted to correlate critical structure doses to erectile dysfunction following the implant. Early work by DiBiase showed a weak correlation between impotence and dose to the neurovascular bundles (NVB) (DiBiase et al., 2000). The NVB are not readily seen in CT images so a surrogate location for these structures was used. This location was based upon prostatic border delineation, adding another layer of uncertainty to the position of the NVB. Other, similar studies were unable to substantiate this correlation (Merrick et al., 2000b). Stock was able to correlate D_{90} values to erectile dysfunction, but it is doubtful that the gland itself is the critical structure in this regard. It is more likely that the high doses delivered to the prostate were correlates to high doses to some other critical structure. In any case, keeping D_{90} less than 160 Gy for iodine and 100 Gy for palladium monotherapy were recommended in their results (Stock, Kao, and Stone 2001). A strong correlation was noted between impotence and excessive dose to the penile bulb. The penile bulb lies 1 to 2 cm inferior to the apex of the prostate gland. It has been strongly recommended that the dose to 50% of this structure, D_{50}, be kept below 50 Gy. Most implant design techniques employed today easily achieve this recommendation (Merrick et al., 2001, 2002).

Post-Implant Targets

Table 3 lists suggested implant evaluation targets for PPB based upon the listed references. It should be noted that these targets are highly subjective and include the author's bias. They should be tailored to the needs of the brachytherapist and the practice. Balancing the optimal chance for a cure against the risk of complications for the individual patient is the art of medicine, always within the realm of the patient's physician.

The Post-Implant Evaluation Program

A post-implant evaluation should be conducted for each patient. Target coverage and dose to critical structures should be calculated and evaluated in terms of implant targets, like those in Table 3, which have been set by the brachytherapist and modified according to the patient's needs. A practitioner who has never had a suboptimal implant has never looked. Such implants should be evaluated for additional intervention in the case of inadequate coverage, or for added therapeutic intervention or increased follow up and monitoring in the case of excessive doses to critical structures (Yu et al., 1999; Nag et al. 2000, 2002).

Reporting

Suggested post-implant reporting formats vary according to the type of implant. In addition to the demographic data, as a minimum each implant evaluation report should contain the type of implant, the target volume—as formulated in International Commission on Radiation Units and measurements (ICRU) reports 50 and 62, if possible, a description of the target and implanted volume; a description of the implant plan, to include the type and form of sources, the air kerma strength; and an evaluation of the implant results, a description of the dose to the target and to the critical structures (Anderson et al., 1991; Nath et al., 1997). Several dedicated prostate brachytherapy treatment-planning systems offer automated report generation; this can reduce dramatically the amount of time required. Table 4 lists the recommended report-

Table 3. Suggested Post-Implant Dosimetry Targets

Structure	Intent	Goal	References
Prostate Gland	Cure	D_{90} for iodine monotherapy > 140 Gy D_{90} for palladium monotherapy > 125 Gy D_{90} for boosts > reference dose	Stock et al. (1998) Potters et al. (2001)
Prostate Gland	Urethral complications	D_{90} < 180 Gy V_{150} < 60% reference dose	Stock and Stone (2002) Merrick et al. (2002)
Membranous Urethra	Urethral complications	Dose to the membranous urethra < reference dose	Merrick et al. (2002)
Rectum	Rectal complications	Dose to > 1 cm length of anterior mucosal wall < reference dose Max dose to anterior mucosal wall < 120% of reference dose	Merrick et al. (1999a)
Rectum	Rectal complications	Annular DVH of rectum < 1.3 cm^3 to 160 Gy (iodine)	Snyder et al. (2001)
Rectum	Rectal complications	Surface area of outer rectal wall < 5 cm^2 to reference dose	Han and Wallner (2001)

Table 4. Suggested Reporting Formats

Brachytherapy procedure	Reporting format
Gynecological brachytherapy	ICRU 38
Gynecological brachytherapy (HDR)	ICRU 38, Nag et al. (2000)
Interstitial implants	ICRU 58
Prostate brachytherapy	Gillin 1990, Yu et al. (1999), Nag et al. (2002)
General Bbrachytherapy	Anderson et al. (1991), Nath et al. (1997)

ing formats for several implant types. A suggested format for prostate brachytherapy implants is attached as an appendix.

Compiling these results into a useful format for analyzing a series of implants can be quite cumbersome. Due to the popularity of the procedure, software that automatically downloads and stores the implant descriptors in a database is available for prostate brachytherapy; compiling the results for other types of implants has yet to reach this level of ease.

Program Review

A review of the implant program should be performed at least annually (Nath et al., 1997; Nag et al. 2000). Additional reviews may be conducted following the introduction of a new technique or a change of equipment (Bice, Prestidge, and Sarosdy 2001).

Program reviews can be very useful in guiding the implant team into taking the necessary steps to improve implant quality. While there is no specific format for this review, suggestions have been made in regulatory documents with regard to the adequacy of record keeping (U.S. NRC 1991). Such analysis is useful, of course, but does little to improve the performance of the implant team in achieving better implants. In this regard the review should include an analysis of implant dosimetry quantifiers and how well these quantifiers achieve the stated goals. These quantifiers should not be limited to target coverage but should also include dosimetry information pertaining to critical structures.

Additionally, some sort of tracking with regard to clinical outcome is extremely useful. While it is impractical to expect most implant programs to maintain a full database with regard to patient follow-up, tracking a single type of complication and attempting to draw a correlation to the post-implant dosimetry is both possible and useful. For instance, knowing which patients had urinary complications following prostate brachytherapy allows the practitioner to focus on the dosimetry for these patients and to determine how the implant characteristics for these patients differ from the rest. Quantifiers to focus first might be those listed in Table 3, or other correlates for urinary complications—D_{90} values, for instance. It is also possible to choose other dosimetric characteristics to analyze, dose to the bladder neck or number of needle passes, for example.

Of course, the evaluation is not the goal; we hope for better implants. Improving implant performance can be achieved only if the results are critically analyzed by the implant team members. Changing implant design, equipment, or delivery techniques should all be considered in order to improve. The implant team needs to digest and learn from this type of evaluation, possible only when egos are swallowed and frank discussion ensues. This sort of analysis can become difficult and entail hard work, but the results can be quite dramatic.

Multicenter Trials

Multicenter trials are essential to the advancement of medical knowledge. These trials have been performed using post-implant evaluation results (Bice et al., 1998; Wallner et al., 2002; Al-Qaisieh 2003; Mangili et al., 2004). Such studies are especially difficult due to the uncertainties associated with target and critical structure delineation. The lack of a standard protocol for calculating and analyzing dosimetry results is also problematic. The quality control for research protocols that rely on post-implant evaluation to categorize and compare results often must be quite detailed, rely on extensive over reading of subjective interpretation, and require centralized data storage and analysis (RTOG 2002).

Summary

In that the results can affect more than just a single implant, post-implant evaluation may be considered the most critical element of the brachytherapy procedure. Skipping this evaluation is dangerous for the patient and for the implant program (Stock and Stone 2002). It is truly impossible to deliver high-quality care consistently without an aggressive evaluation program. The basis for any brachytherapy evaluation program is the post plan.

Post-implant evaluation provides the foundation upon which our current knowledge base is laid. Only by looking at the results from large series of implants have we been able to make sense of clinical outcomes. How the implant procedure is performed does make a difference.

Problems do exist. There is no perfect imaging modality; what works well for delineating the soft tissues is notoriously poor at localizing the sources; and vice versa. Combining imaging modalities has the added uncertainty associated with image co-registration and is expensive.

Our analytical tools are admittedly immature. Modern calculation methods and treatment planning systems have been available for less than 10 years. Which quantifiers are valuable and how they relate to clinical outcomes will continue to be the subject of study for many years. Analysis and display methods are nonstandard; which tier on the post-implant evaluation hierarchy is appropriate for evaluation of dosimetry will continue to be a matter of debate.

Three or four years ago there was a noticeable shift of the focus of clinical studies from cures to complications. This is highly encouraging, indicative of a satisfaction with our ability to cure the disease, concentrating instead on how to make the procedure less morbid. We know we deliver better implants, but how much better we can get and whether this improvement in quality can be generally attained remain uncertain.

Appendix. Sample Reporting Format for Permanent Prostate Brachytherapy

Brachytherapy Report Date: Wednesday, January 1, 2000

Patient: Mr. Truly Anonymous, MR#00001
Physician: Frank Lee Neerdowell, MD

General

On Tuesday, November 14, 1999 an ultrasound volume study was performed on Mr. Anonymous following a biopsy positive for prostate cancer. From this ultrasound study, the size and location of the prostate gland was determined and a radioactive implant (brachytherapy) using iodine-125 (GreedySeedVendorModel)(NIST99) radioactive sources was planned. Usually termed a preplan, this treatment plan was used to guide the placement of seeds in the operating room during the implant procedure performed on Thursday, December 1, 1999. During the implant procedure 106 sources of iodine-125 (GreedySeedVendorModel) (NIST99) were implanted in and around the prostate with the intent of delivering a curative dose of radiation to the gland. Subsequently, on Thursday, December 15, 1999, a CT scan was performed to evaluate the quality of the implant; by noting the position of the seeds a dosimetric evaluation of the implant was conducted. This treatment plan is termed a "post plan" in that it was performed after the procedure.

Description of Volumes

Mr. Anonymous has clinical stage T1c adenocarcinoma of the prostate, a Gleason sum score of 6/10, and a pre-implant prostate specific antigen level of 4.6 ng/ml. The gross tumor volume includes the left apex and left base of the prostate gland, which were positive from the biopsy. The clinical target volume is the entire prostate gland, which had a volume of 43.1 cm^3 based upon the ultrasound volume study. The planning volume extends several millimeters outside the gland lateral and anterior with a larger margin at the base and apex of the gland than in the central regions. The posterior margin of the PTV is smaller to minimize rectal dose.

Sources and Techniques

GreedySeedVendor I125 sources, model GSVModel#, were used to perform the implant. The implemented preplan consisted of an array of 24 needles with a total of 104 sources arranged to deliver dose in as uniform a pattern as possible throughout the planning target volume. Most needles had sources placed at 10 mm spacing, the exceptions being at the periphery of the gland, particularly at the base and apex, to ensure adequate dosimetric coverage. The implant design technique is termed "modified-peripheral" with the exact locations detailed in the loading map attached to the preplan. The source positions used in this implant were uniquely designed for this patient in conjunction with the physician's desire to achieve a specific dose distribution.

The implant was carried out with 2 extra sources. The reason that extra sources were implanted was based upon the perceived source distribution at the end of the implant procedure as determined via fluoroscopy. The total number of sources implanted was 106. 105, I-125 (GreedySeedVendor) (NIST99) sources of 0.34 mCi (0.429 U) each were used in the post plan evaluation. This number was derived from an AP radiograph with exact locations determined from the CT scan.

Total Reference Air Kerma

At the time of the implant the total reference air kerma rate for this implant was 45.50 microGy per hour at 1 meter. Source strength was verified by assay to within 5% of this value by using an independent measuring system that has a calibration traceable to the National Institute for Standards and Technology.

Description of the Dose Distribution

The prescribed dose for this implant was 145 Gy. Sometimes termed the "reference dose," this is the minimum dose to be achieved in the design of the implant (or preplan). Isodose curves and dose volume histograms (DVHs) attached to the preplan illustrate this. The achieved dose distribution is detailed in the post plan isodose display and DVHs. Because of post-implant edema and uncertainties in the delineation of the prostatic volume on CT, the resultant doses are best described in terms of several quantifiers generated form analysis of the DVH. The percentage of the gland that received 100% of the reference dose or greater, termed V_{100}, for this implant was 96.7%. Similarly, that percentage of the gland that received 80% of the reference dose or greater, V_{80}, was 99.8%.

D_{90}, or the lowest dose that covers 90% of the gland, is 167 Gy.

With regard to uniformity, the dose non-uniformity ratio (DNR) for this implant was 0.471. This is the ratio of the tissue volume that received 150% or greater of the reference dose divided by the volume that received 100% of the reference dose or greater. The DNR is a measure of the uniformity of the implant with a range from 0 to 1, smaller numbers indicative of a more uniform dose distribution. The DNR is independent of prostate volume. It is a possible indicator of the chance of complications and is used in the same manner as V_{150}, which was 55.2% for this implant.

A urethra dose trace (dose along the center of the urethra) is provided in the post plan as is a dose surface histogram of the urethral wall. These indicate that none of the urethra received more than 200% of the reference dose and none received more than 250% of the reference dose. The dose to the bladder neck is estimated to be 113 Gy.

A DSH of the rectum indicates that 2.78 square centimeters of the rectum wall received 100% of the reference dose or greater. Similarly, 0.05 square centimeters of the rectal wall received 150% of the reference dose or greater.

Submitted:

_____

William S. Bice, Jr., Ph.D., CSMP
Medical Physicist

Reviewed by:

_____

Frank Lee Neerdowell, MD
Radiation Oncologist

References

Al-Qaisieh, B. (2003). "Pre- and post-implant dosimetry: An inter-comparison between UK prostate brachytherapy centres." *Radiother Oncol* 66(2):181-183.

Amdur, R. J., D. Gladstone, K. A. Leopold, and R. D. Harris. (1999). "Prostate seed implant quality assessment using MR and CT image fusion." *Int J Radiat Oncol Biol Phys* 43(1):67–72.

Anagnostopoulos, G., D. Baltas, A. Geretschlaeger, T. Martin, P. Papagiannis, N. Tselis, and N. Zamboglou. (2003). "In vivo thermoluminescence dosimetry dose verification of transperineal ^{192}Ir high-dose-rate brachytherapy using CT-based planning for the treatment of prostate cancer." *Int J Radiat Oncol Biol Phys* 57(4):1183–1191.

Anderson, L. L. (1986). "A 'natural' volume-dose histogram for brachytherapy." *Med Phys* 13:898–903.

Anderson, L., R. Nath, A. J. Olch, and J. Roy. (1991). "American Endocurietherapy Society recommendations for dose specification in brachytherapy." *Endocuriether/Hypertherm Oncol* 7:1–12.

Badiozamani, K. R., K. Wallner, W. Cavanagh, and J. Blasko. (1999). "Comparability of CT-based and TRUS-based prostate volumes." *Int J Radiat Oncol Biol Phys* 43(2):375–378.

Beaulieu, L., L. Archambault, S. Aubin, E. Oral, R. Taschereau, and J. Pouliot. (2004~~a~~). "The robustness of dose distributions to displacement and migration of ^{125}I permanent seed implants over a wide range of seed number, activity, and designs." *Int J Radiat Oncol Biol Phy*s 58:1298–1308.

Bice, W. S., Jr., B. R. Prestidge, and M. F. Sarosdy. (2001). "Sector analysis of prostate implants." *Med Phys* 28(12):2561–2567.

Bice, W. S., Jr., B. R. Prestidge, P. D. Grimm, J. L. Friedland, V. Feygelman, M. Roach 3rd, J. J. Prete, D. F. Dubois, and J. C. Blasko. (1998). "Centralized multiinstitutional postimplant analysis for interstitial prostate brachytherapy." *Int J Radiat Oncol Biol Phys* 41(4): 921–927.

Bice, W. S., Jr., D. F. Dubois, J. J. Prete, and B. R. Prestidge. (1999). "Source localization from axial image sets by iterative relaxation of the nearest neighbor criterion." *Med Phys* 26(9):1919–1924.

Bice, W. S., Jr., J. E. Freeman, L. F. Russell, Jr., G. D. Case, D. F. Dubois, J. J. Prete, and B. R. Prestidge. (2000). "Use of image coregistration in salvage prostate brachytherapy." *Tech Urol* 6(2):151–156.

Brinkmann, D., and R. W. Kline. (1998). "Automated seed localization from CT datasets of the prostate." *Med Phys* 25(9):1667–1672.

Butler, W. M., G. S. Merrick, A. T. Dorsey, and B. M. Hagedorn. (2000a). "Comparison of dose length, area, and volume histograms as quantifiers of urethral dose in prostate brachytherapy." *Int J Radiat Oncol Biol Phys* 48(5):1575–1582.

Butler, W. M., G. S. Merrick, A. T. Dorsey, and J. H. Lief. (2000b). "Isotope choice and the effect of edema on prostate brachytherapy dosimetry." *Med Phys* 27(5):1067–1075.

Claus, F. G., H. Hricak, and R. R. Hattery. (2004). "Pretreatment evaluation of prostate cancer: Role of MR imaging and 1H MR spectroscopy." *Radiographics* 24(Suppl 1):S167–S180.

Crook, J., M. Milosevic, P. Catton, I. Yeung, T. Haycocks, T. Tran, C. Catton, M. McLean, T. Panzarella, and M. A. Haider. (2002). "Interobserver variation in postimplant computed tomography contouring affects quality assessment of prostate brachytherapy." *Brachytherapy* 1(2):66–73.

D'Amico, A., R. Cormack, S. Kumar, and C. M. Tempany. (2000). "Real-time magnetic resonance imaging-guided brachytherapy in the treatment of selected patients with clinically localized prostate cancer." *J Endourol* 14(4):367–370.

Davis, B. J., Brinkmann, D. H., Kruse, J. J., Herman, M. G., LaJoie, W. N., Schwart, D. J., Pisansky, T. M., and R. W. Kline. (2004). "Selective identification of different brachytherapy sources, ferromagnetic seeds, and fiducials in the prostate using an automated seed sorting algorithm." *Brachytherapy* 3:106–112.

DeWyngaert, J. K., M. E. Noz, B. Ellerin, E. L. Kramer, G. Q. Maguire Jr., and M. P. Zeleznik. (2004). "Procedure for unmasking localization information from ProstaScint scans for prostate radiation therapy treatment planning." *Int J Radiat Oncol Biol Phys* 60(2):654–662.

Desai, J., R. G. Stock, N. N. Stone, C. Iannuzzi, and J. K. DeWyngaert. (1998). "Acute urinary morbidity following I-125 interstitial implantation of the prostate gland." *Radiat Oncol Investig* 6(3):135–141.

DiBiase, S. J., K. Wallner, K. Tralins, and S. Sutlief. (2000). "Brachytherapy radiation doses to the neurovascular bundles." *Int J Radiat Oncol Biol Phys* 46(5):1301–1307.

Dogan, N., N. Mohideen, G. P. Glasgow, K. Keys, and R. C. Flanigan. (2002). "Effect of prostatic edema on CT-based postimplant dosimetry." *Int J Radiat Oncol Biol Phys* 53(2):483–489.

Dubois, D. F. (1999). Magnetic Resonance Imaging in Permanent Prostate Brachytherapy. Department of Radiology. San Antonio, Texas, University of Texas Health Science Center at San Antonio.

Dubois, D. F., W. S. Bice Jr., and B. R. Prestidge. (2001). "CT and MRI derived source localization error in a custom prostate phantom using automated image coregistration." *Med Phys* 28(11):2280–2284.

Dubois, D. F., B. R. Prestidge, L. A. Hotchkiss, W. S. Bice Jr., and J. J. Prete. (1997). "Source localization following permanent transperineal prostate interstitial brachytherapy using magnetic resonance imaging." *Int J Radiat Oncol Biol Phys* 39(5):1037–1041.

Dubois, D. F., B. R. Prestidge, L. A. Hotchkiss, J. J. Prete, and W. S. Bice Jr. (1998). "Intraobserver and interobserver variability of MR imaging- and CT-derived prostate volumes after transperineal interstitial permanent prostate brachytherapy." *Radiology* 207(3):785–789.

Ellis, R. J., E. Kim, and R. Foor. (2004). "Role of ProstaScint for brachytherapy in localized prostate adenocarcinoma." *Expert Rev Mol Diagn* 4(4):435–441.

Ellis, R. J., A. Vertocnik, E. Kim, H. Zhou, B. Young, B. Sodee, P. Fu, S. Beddar, V. Colussi, J. P. Spirnak, K. H. Dinchman, M. Resnick, and T. J. Kinsella. (2003). "Four-year biochemical outcome after radioimmunoguided transperineal brachytherapy for patients with prostate adenocarcinoma." *Int J Radiat Oncol Biol Phys* 57(2):362–370.

Fang, D. X., R. G. Stock, N. N. Stone, B. R. Krynyckyi, C. K. Kim, and J. Machac. (2000). "Use of radioimmunoscintigraphy with indium-111-labeled CYT-356 (ProstaScint) scan for evaluation of patients for salvage brachytherapy." *Tech Urol* 6(2):146–150.

Fuller, D. B., J. A. Koziol, and A. C. Feng. (2004). "Prostate brachytherapy seed migration and dosimetry: analysis of stranded sources and other potential predictive factors." *Brachytherapy* 3(1):10–19.

Gillin, M.T., D.L. Zellmer, D.F. Grimm and K. Sherwood. (1992). "Practical Considerations for Interstitial Brachytherapy" in *Advances in Radiation Oncology Physics, Dosimetry, Treatment Planning and Brachytherapy.* J. A. Purdy (ed.). AAPM Medical Physics Monograph Number 19. New York: American Institute of Physics, pp. 703-727, 1992.

Gong, L., P. S. Cho, B. H. Han, K. E. Wallner, S. G. Sutlief, S. D. Pathak, D. R. Haynor, and Y. Kim. (2002). "Ultrasonography and fluoroscopic fusion for prostate brachytherapy dosimetry." *Int J Radiat Oncol Biol Phys* 54(5):1322–1330.

Han, B. H., and K. E. Wallner. (2001). "Dosimetric and radiographic correlates to prostate brachytherapy-related rectal complications." *Int J Cancer* 96(6):372–378.

Han, B. H., K. Wallner, G. Merrick, K. Badiozamani, and W. Butler. (2003a). "The effect of interobserver differences in post-implant prostate CT image interpretation on dosimetric parameters." *Med Phys* 30(6):1096–1102.

Han, B. H., K. Wallner, G. Merrick, W. Butler, S. Sutlief, and J. Sylvester. (2003b). "Prostate brachytherapy seed identification on post-implant TRUS images." *Med Phys* 30(5):898–900.

Hilts, M., I. Spadinger, and M. Keyes. (2002). "Comparison of methods for calculating rectal dose after ^{125}I prostate brachytherapy implants." *Int J Radiat Oncol Biol Phys* 53(3):775–785.

Holmes, D. R., 3rd, B. J. Davis, and R. A. Robb. (2001). "3D localization of implanted radioactive sources in the prostate using trans-urethral ultrasound." *Stud Health Technol Inform* 81:199–205.

Holupka, E. J., P. M. Meskell, E. C. Burdette, and I. D. Kaplan. (2004). "An automatic seed finder for brachytherapy CT postplans based on the Hough transform." *Med Phys* 31(9):2672–2679.

International Commission on Radiation Units and Measurements (ICRU). Report No. 38. "Dose and Volume Specification for Reporting Intracavitary Therapy in Gynecology." Bethesda, MD: ICRU, 1985.

International Commission on Radiation Units and Measurements (ICRU). Report No. 50. "Prescribing, Recording and Reporting Photon Beam Therapy." Bethesda, MD: ICRU, 1993.

International Commission on Radiation Units and Measurements (ICRU). Report No. 58. "Dose and Volume Specification for Reporting Interstitial Therapy." Bethesda, MD: ICRU, 1997.

International Commission on Radiation Units and Measurements (ICRU). Report No. 62: "Prescribing, Recording and Reporting Photon Beam Therapy (Supplement to ICRU Report 50)." Bethesda, MD: ICRU, 1999.

Karouzakis, K., M. Lahanas, N. Milickovic, S. Giannouli, D. Baltas. and N. Zamboglou. (2002). "Brachytherapy dose-volume histogram computations using optimized stratified sampling methods." *Med Phys* 29(3):424–432.

Kooy, H. M., R. A. Cormack, G. Mathiowitz, C. Tempany, and A. V. D'Amico. (2000). "A software system for interventional magnetic resonance image-guided prostate brachytherapy." *Comput Aided Surg* 5:401–413.

Lam, S. T., P. S. Cho, R. J. Marks II, and S. Narayanan. (2004). "Three-dimensional seed reconstruction for prostate brachytherapy using Hough trajectories." *Phys Med Biol* 49(4):557–569.

Lee, W. R., M. Roach 3rd, J. Michalski, B. Moran, and D. Beyer. (2002). "Interobserver variability leads to significant differences in quantifiers of prostate implant adequacy." *Int J Radiat Oncol Biol Phys* 54(2):457–461.

Li, Z., I. A. Nalcacioglu, S. Ranka, S. K. Sahni, J. R. Palta, W. Tome, and S. Kim. (2001). "An algorithm for automatic, computed-tomography-based source localization after prostate implant." *Med Phys* 28(7):1410–1415.

Lindsay, P. E., J. Van Dyk, and J. J. Battista. (2003). "A systematic study of imaging uncertainties and their impact on ^{125}I prostate brachytherapy dose evaluation." *Med Phys* 30(7):1897–1908.

Ling, C. C., J. Roy, N. Sahoo, K. Wallner, and L. Anderson. (1994). "Quantifying the effect of dose inhomogeneity in brachytherapy: Application to permanent prostatic implant with ^{125}I seeds." *Int J Radiat Oncol Biol Phys* 28(4):971–978.

Liu, H., G. Cheng, Y. Yu, R. Brasacchio, D. Rubens, J. Strang, L. Liao, and E. Messing. (2003). "Automatic localization of implanted seeds from postimplant CT images." *Phys Med Biol* 48:1191–1203.

Lu, X. Q., and L. M. Chin. (1993). "Sampling techniques for the evaluation of treatment plans." *Med Phys* 20(1):151–161.

Mangili, P., L. Stea, F. Cattani, S. Lappi, F. Giglioli, E. Calamia, F. Ziglio, R. Martinelli, and B. Longobardi. (2004). "Comparative study of permanent interstitial prostate brachytherapy post-implant evaluation among seven Italian institutes." *Radiother Oncol* 71(1):13–21.

McLaughlin, P. W., V. Narayana, D. G. Drake, B. M. Miller, L. Marsh, J. Chan, R. Gonda Jr., R. J. Winfield, and P. L. Roberson. (2002). "Comparison of MRI pulse sequences in defining prostate volume after permanent implantation." *Int J Radiat Oncol Biol Phys* 54(3):703–711.

McLaughlin, P. W., V. Narayana, A. Meriowitz, S. Troyer, P. L. Roberson, R. Gonda Jr., H. Sandler, L. Marsh, T. Lawrence, and M. Kessler. (2005). "Vessel-sparing prostate radiotherapy: dose limitation to critical erectile vascular structures (internal pudendal artery and corpus cavernosum) defined by MRI." *Int J Radiat Oncol Biol Phys* 61(1):20–31.

Merrick, G. S., and W. M. Butler, (2004). "Rectal function following permanent prostate brachytherapy." *W V Med J* 100(1):18–20.

Merrick, G. S., W. M. Butler, A. T. Dorsey, and H. L. Walbert. (1998). "Influence of timing on the dosimetric analysis of transperineal ultrasound-guided, prostatic conformal brachytherapy." *Radiat Oncol Investig* 6(4):182–190.

Merrick, G. S., W. M. Butler, A. T. Dorsey, J. H. Lief, H. L. Walbert, and H. J. Blatt. (1999a). "Rectal dosimetric analysis following prostate brachytherapy." *Int J Radiat Oncol Biol Phys* 43(5):1021–1027.

Merrick, G. S., W. M. Butler, A. T. Dorsey, and J. H. Lief. (1999b). "The dependence of prostate postimplant dosimetric quality on CT volume determination." *Int J Radiat Oncol Biol Phys* 44(5):1111–1117.

Merrick, G. S., W. M. Butler, A. T. Dorsey, J. H. Lief, and M. L. Benson. (2000a). "Seed fixity in the prostate/periprostatic region following brachytherapy." *Int J Radiat Oncol Biol Phys* 46(1):215–220.

Merrick, G. S., W. M. Butler, A. T. Dorsey, J. H. Lief, and J. G. Donzella. (2000b). "A comparison of radiation dose to the neurovascular bundles in men with and without prostate brachytherapy-induced erectile dysfunction." *Int J Radiat Oncol Biol Phys* 48(4):1069–1074.

Merrick, G. S., K. Wallner, R. W. Galbreath, J. H. Lief, and M. L. Benson. (2001). "A comparison of radiation dose to the bulb of the penis in men with and without prostate brachytherapy-induced erectile dysfunction." *Int J Radiat Oncol Biol Phys* 50(3):597–604.

Merrick, G. S., W. M. Butler, K. E. Wallner, J. H. Lief, R. L. Anderson, B. J. Smeiles, R. W. Galbreath, and M. L. Benson. (2002). "The importance of radiation doses to the penile bulb vs. crura in the development of postbrachytherapy erectile dysfunction." *Int J Radiat Oncol Biol Phys* 54(4):1055–1062.

Mizowaki, T., G. N. Cohen, A. Y. Fung, and M. Zaider. (2002). "Towards integrating functional imaging in the treatment of prostate cancer with radiation: the registration of the MR spectroscopy imaging to ultrasound/CT images and its implementation in treatment planning." *Int J Radiat Oncol Biol Phys* 54(5):1558–1564.

Moerland, M. A., H. K. Wijrdeman, R. Beersma, C. J. Bakker, and J. J. Battermann. (1997). "Evaluation of permanent I-125 prostate implants using radiography and magnetic resonance imaging." *Int J Radiat Oncol Biol Phys* 37(4):927–933.

Moerland, M. A., R. van der Laarse, R. W. Luthmann, H. K. Wijderman, and J. J. Battermann. (2000). "The combined use of the natural and the cumulative dose-volume histograms in planning and evaluation of permanent prostatic seed implants." *Radiother Oncol* 57:279–284.

Nag, S., W. Bice, K. DeWyngaert, B. Prestidge, R. Stock, R., and Y. Yu. (2000). "The American brachytherapy society recommendations for permanent prostate brachytherapy postimplant dosimetric analysis." *Int J Radiat Oncol Biol Phys* 46:221–230.

Nag, S., R. J. Ellis, S. Merrick, R. Bahnson, K. Wallner, and R. Stock. (2002). "American Brachytherapy Society recommendations for reporting morbidity after prostate brachytherapy." *Int J Radiat Oncol Biol Phys* 54(2):462–470.

Narayana, V., P. L. Roberson, R. J. Winfield, and P. W. McLaughlin. (1997). "Impact of ultrasound and computed tomography prostate volume registration on evaluation of permanent prostate implants." *Int J Radiat Oncol Biol Phys* 39(2):341–346.

Narayanan, S., P. S. Cho, and R. J. Marks II. (2004). "Three-dimensional seed reconstruction from an incomplete data set for prostate brachytherapy." *Phys Med Biol* 49(15):3483–3494.

Nath, R., L. L. Anderson, G. Luxton, K. A. Weaver, J. F. Williamson, and A. S. Meigooni. (1995). "Dosimetry of interstitial brachytherapy sources: Recommendations of the AAPM Radiation Therapy Committee, Task Group No. 43." *Med Phys* 22:209–234. Also available as AAPM Report No. 51.

Nath, R., L. L. Anderson, J. A. Meli, A. J. Olch, J. A. Stitt, and J. F. Williamson. (1997). "Code of practice for brachytherapy physics: Report of the AAPM Radiation Therapy Committee Task Group No. 56." *Med Phys* 24(10):1557–1598. Also available as AAPM Report No. 59.

Niemierko, A., and M. Goitein. (1994). "Dose-volume distributions: A new approach to dose-volume histograms in three-dimensional treatment planning." *Med Phys* 21(1):3–11.

Polo, A., F. Cattani, A. Vavassori, D. Origgi, G. Villa, H. Marsiglia, M. Bellomi, G. Tosi, O. De Cobelli, and R. Orecchia. (2004). "MR and CT image fusion for postimplant analysis in permanent prostate seed implants." *Int J Radiat Oncol Biol Phys* 60(5):1572–1579.

Potters, L., Y. Cao, E. Calugaru, T. Torre, P. Fearn, and X. H. Wang. (2001). "A comprehensive review of CT-based dosimetry parameters and biochemical control in patients treated with permanent prostate brachytherapy." *Int J Radiat Oncol Biol Phys* 50(3):605–614.

Prestidge, B. R., W. S. Bice, E. J. Kiefer, and J. J. Prete. (1998). "Timing of computed tomography-based postimplant assessment following permanent transperineal prostate brachytherapy." *Int J Radiat Oncol Biol Phys* 40(5):1111–1115.

Prete, J. J., B. R. Prestidge, W. S. Bice, D. F. Dubois, and L. A. Hotchkiss. (1998). "Comparison of MRI- and CT-based post-implant dosimetric analysis of transperineal interstitial permanent prostate brachytherapy." *Radiat Oncol Investig* 6(2):90–96.

Radiation Therapy Oncology Group (RTOG) P0232 (2002). "A phase III study comparing combined external beam radiation and transperineal interstitial permanent brachytherapy with brachytherapy alone for selected patients with intermediate risk prostatic carcinoma." B. Prestidge, (Principal Investigator).

Rivard, M. J., B. M. Coursey, L. A. DeWerd, W. F. Hanson, M. S. Huq, G. S. Ibbott, M. G. Mitch, R. Nath, and J. F. Williamson. (2004). "Update of AAPM Task Group No. 43 Report: A revised AAPM protocol for brachytherapy dose calculations." *Med Phys* 31:633–674. Also available as AAPM Report No. 84.

Roberson, P. L., V. Narayana, D. L. McShan, R. J. Winfield, and P. W. McLaughlin. (1997). "Source placement error for permanent implant of the prostate." *Med Phys* 24(2):251–257.

Roy, J. N., L. L. Anderson, K. E. Wallner, Z. Fuks, and C. C. Ling. (1993). "Tumor control probability for permanent implants in prostate." *Radiother Oncol* 28(1):72–75.

Roy, J. N., K. E. Wallner, P. J. Harrington, C. C. Ling, and L. L. Anderson. (1993). "A CT-based evaluation method for permanent implants: application to prostate." *Int J Radiat Oncol Biol Phys* 26(1):163–169.

Sajo, E. (2003). Private communication. The use of PET to localize sources in permanent prostate brachytherapy. W. Bice. Baton Rouge, LA.

Saw, C. B., and N. Suntharalingam. (1991). "Quantitative assessment of interstitial implants." *Int J Radiat Oncol Biol Phys* 20(1):135–139.

Smith, S., K. Wallner, G. Merrick, W. Butler, S. Sutlief, and P. Grimm. (2003). "Interpretation of pre- versus postimplant TRUS images." *Med Phys* 30(5):920–924.

Snyder, K. M., R. G. Stock, S. M. Hong, Y. C. Lo, and N. N. Stone. (2001). "Defining the risk of developing grade 2 proctitis following 125I prostate brachytherapy using a rectal dose-volume histogram analysis." *Int J Radiat Oncol Biol Phys* 50(2):335–341.

Sodee, D. B., R. J. Ellis, M. A. Samuels, J. P. Spirnak, W. F. Poole, C. Riester, D. M. Martanovic, R. Stonecipher, and E. M. Bellon. (1998). "Prostate cancer and prostate bed SPECT imaging with ProstaScint: Semiquantitative correlation with prostatic biopsy results." *Prostate* 37(3):140–148.

Speight, J., K. Shinohara, B. Pickett, V. Weinberg, I.-C. Hsu, and M. Roach III. (2000). "Prostate volume change after radioactive seed implantation: Possible benefit of improved dose volume histogram with perioperative steroid." *Int J Radiat Oncol Biol Phys* 48(5):1461–1467.

Stock, R. G., and N. N. Stone. (2002). "Importance of post-implant dosimetry in permanent prostate brachytherapy." *Eur Urol* 41(4):434–439.

Stock, R. G., J. Kao, and N. N. Stone. (2001). "Penile erectile function after permanent radioactive seed implantation for treatment of prostate cancer." *J Urol* 165(2):436–439.

Stock, R. G., N. N. Stone, A. Tabert, C. Iannuzzi, and J. K. DeWyngaert. (1998). "A dose-response study for I-125 prostate implants." *Int J Radiat Oncol Biol Phys* 41(1):101–108.

Su, Y., B. J. Davis, M. G. Herman, and R. A. Robb. (2004). "Prostate brachytherapy seed localization by analysis of multiple projections: Identifying and addressing the seed overlap problem." *Med Phys* 31(5):1277–1287.

Texter, J. H., Jr., and C. E. Neal. (1998). "The role of monoclonal antibody in the management of prostate adenocarcinoma." *J Urol* 160(6 Pt 2):2393–2395.

Tsai, A., W. Wells, C. Tempany, E. Grimson, and A. Willsky. (2004). "Mutual information in coupled multi-shape model for medical image segmentation." *Med Image Anal* 8(4):429–445.

Tubic, D., A. Zaccarin, J. Pouliot, and L. Beaulieu. (2001a). "Automated seed detection and three-dimensional reconstruction. I. Seed localization from fluoroscopic images or radiographs." *Med Phys* 28:2265–2271.

Tutar, I. B., R. Managuli, V. Shamdasani, P. S. Cho, S. D. Pathak, and Y. Kim. (2003). "Tomosynthesis-based localization of radioactive seeds in prostate brachytherapy." *Med Phys* 30(12):3135–3142.

U.S. Nuclear Regulatory Commission. (1991). Regulatory Guide 8.33, Quality Management Program. Washington D.C.: Nuclear Regulatory Commission.

Wallner, K., J. Roy, L. True, W. Cavanagh, C. Simpson, and W. Butler. (1995). "Dosimetry guidelines to minimize urethral and rectal morbidity following transperineal I-125 prostate brachytherapy." *Int J Radiat Oncol Biol Phys* 32(2):465–471.

Wallner, K., G. Merrick, L. True, W. Cavanaugh, C. Simpson, and W. Butler. (2002). "I-125 versus Pd-103 for low-risk prostate cancer: morbidity outcomes from a prospective randomized multicenter trial." *Cancer J* 8(1):67–73.

Waterman, F. M., and A. P. Dicker. (1999). "Effect of post-implant edema on the rectal dose in prostate brachytherapy." *Int J Radiat Oncol Biol Phys* 45(3):571–576.

Waterman, F. M., and A. P. Dicker. (2000). "The impact of postimplant edema on the urethral dose in prostate brachytherapy." *Int J Radiat Oncol Biol Phys* 47(3):661–664.

Willins, J., and K. Wallner. (1997). "CT-based dosimetry for transperineal I-125 prostate brachytherapy." *Int J Radiat Oncol Biol Phys* 39(2):347–353.

Willins, J., and K. Wallner. (1998). "Time-dependent changes in CT-based dosimetry of I-125 prostate brachytherapy." *Radiat Oncol Investig* 6(4):157–160.

Wu, A., K. Ulin, and E. S. Sternick. (1988). "A dose homogeneity index for evaluating ^{192}Ir interstitial breast implants." *Med Phys* 15:104–107.

Wuu, C. S., R. D. Ennis, P. B. Schiff, E. K. Lee, and M. Zaider. (2000). "Dosimetric and volumetric criteria for selecting a source activity and a source type (^{125}I or ^{103}Pd) in the presence of irregular seed placement in permanent prostate implants." *Int J Radiat Oncol Biol Phys* 47:815–820.

Yu, Y., L. L. Anderson, Z. Li, D. E. Mellenberg, R. Nath, M. C. Schell, F. M. Waterman, A. Wu, and J. C. Blasko. (1999). "Permanent prostate seed implant brachytherapy: Report of the American Association of Physicists in Medicine Task Group No. 64." *Med Phys* 26(10):2054–2076. Also available as AAPM Report No. 68.

Yue, N., Z. Chen, R. Peschel, A. P. Dicker, F. M. Waterman, and R. Nath. (1999a). "Optimum timing for image-based dose evaluation of ^{125}I and ^{103}PD prostate seed implants." *Int J Radiat Oncol Biol Phys* 45(4):1063–1072.

Yue, N., A. P. Dicker, B. W. Corn, R. Nath, and F. M. Waterman. (1999b). "A dynamic model for the estimation of optimum timing of computed tomography scan for dose evaluation of ^{125}I or ^{103}Pd seed implant of prostate." *Int J Radiat Oncol Biol Phys* 43(2):447–454.

Yue, N., A. P. Dicker, R. Nath, and F. M. Waterman. (1999c). "The impact of edema on planning ^{125}I and ^{103}Pd prostate implants." *Med Phys* 26(5):763–767.

Zaider, M., M. J. Zelefsky, E. K. Lee, K. L. Zakian, H. I. Amols, J. Dyke, G. Cohen, Y. C. Hu, A. K. Endi, C.-S. Chui, and J. A. Koutcher. (2000). "Treatment planning for prostate implants using magnetic-resonance spectroscopy imaging." *Int J Radiat Oncol Biol Phys* 47(4):1085–1096.